Title
Loss of CDCP1 triggers FAK activation in detached prostate cancer cells.

Journal
American journal of clinical and experimental urology, 9(4)

ISSN
2330-1910

Authors
Pollan, Sara G
Teng, Pai-Chi
Jan, Yu Jen
et al.

Publication Date
2021

Peer reviewed

Am J Clin Exp Urol 2021;9(4):350-366
www.ajceu.us /ISSN:2330-1910/AJCEU0138235

Original Article

Loss of CDCP1 triggers FAK activation in detached prostate cancer cells

Sara G Pollan[1], Pai-Chi Teng[1], Yu Jen Jan[1], Julie Livingstone[2], Cai Huang[3], Minhyung Kim[1], Javier Mariscal[1], Maria Rodriguez[1], Jie-Fu Chen[1], Sungyong You[1], Dolores DiVizio[1], Paul C Boutros[4], Keith Syson Chan[5], Olga Rasorenova[6], Anne Cress[7], Danislav Spassov[8], Mark Moasser[8], Edwin M Posadas[9], Stephen J Freedland[1], Michael R Freeman[1,10], Jie J Zheng[11], Beatrice S Knudsen[10,12]

[1]Department of Surgery, Cedars-Sinai Medical Center, 8700 Beverly Blvd, Los Angeles, CA 90048, USA; [2]Department of Informatics and Biocomputing, Ontario Institute for Cancer Research, Toronto, ON M5G 1L7, Canada; [3]Department of Pharmacology and Nutritional Sciences, Markey Cancer Center, University of Kentucky, 789 South Limestone St, Lexington, KY 40536, USA; [4]Department of Human Genetics and Urology, Jonsson Comprehensive Cancer Centre, University of California, Los Angeles, CA, USA; [5]Department of Pathology, Cedars-Sinai Medical Center, 8700 Beverly Blvd, Los Angeles, CA 90048, USA; [6]Department of Molecular Biology and Biochemistry, University of California Irvine, Irvine, CA 92697, USA; [7]Department of Cellular and Molecular Medicine, University of Arizona College of Medicine, 1501 N, Campbell Avenue, Tucson, AZ 85724, USA; [8]Department of Medicine, University of California San Francisco, San Francisco, CA 94143, USA; [9]Department of Medicine, Cedars-Sinai Medical Center, 8700 Beverly Blvd, Los Angeles, CA 90048, USA; [10]Department of Biomedical Sciences, Cedars-Sinai Medical Center, 8700 Beverly Blvd, Los Angeles, CA 90048, USA; [11]Department of Cell & Developmental Biology, University of California Los Angeles, CHS BH-973B, Los Angeles, CA 90095, USA; [12]Department of Pathology, University of Utah, Salt Lake City, UT 84112, USA

Received August 12, 2021; Accepted August 25, 2021; Epub August 25, 2021; Published August 30, 2021

Abstract: A major metastasis suppressing mechanism is the rapid apoptotic death of cancer cells upon detachment from extracellular matrix, a process called anoikis. Focal adhesion kinase (PTK2/FAK) is a key enzyme involved in evasion of anoikis. We show that loss of the Cub-domain containing protein-1 (CDCP1), paradoxically stimulates FAK activation in the detached state of prostate cancer cells. In CDCP1^{low} DU145 and PC3 prostate cancer cells, detachment-activation of FAK occurs through local production of PI(4,5)P_2. PI(4,5)P_2 is generated by the PIP5K1c-201 splicing isoform of PIP5K1c, which contains a unique SRC phosphorylation site. In the detached state, reduced expression of CDCP1 and an alternative CDCP1-independent SRC activation mechanism triggers PIP5K1c-pY644 phosphorylation by SRC. This causes a switch of Talin binding from β1-integrin to PIP5K1c-pY644 and leads to activation of PIP5K1c-FAK. Reduced CDCP1 expression also inactivates CDK5, a negative regulator of PIP5K1c. Furthermore, immersion of prostate cancer cells in 10% human plasma or fetal bovine serum is required for activation of PIP5K1c-FAK. The PIP5K1c induced detachment-activation of FAK in preclinical models sensitizes CDCP1^{low} prostate cancer cells to FAK inhibitors. In patients, CDCP1^{High} versus CDCP1^{low} circulating tumor cells differ in expression of *AR-v7*, *ONECUT2* and *HOXB13* oncogenes and TMPRSS2 and display intra-patient heterogeneity of FAK-pY397 expression. Taken together, CDCP1^{low} and CDCP1^{high} detached prostate cancer cells activate distinct cytoplasmic kinase complexes and targetable transcription factors, which has important therapeutic implications.

Keywords: CDCP1, prostate cancer metastasis, anoikis, focal adhesion kinase, PIP5K1c

Introduction

Cell adhesion provides a critical survival signal for adherent cancer cells and detachment from extracellular matrix causes rapid cell death through a mechanism called anoikis [1, 2]. In cancer, focal adhesion kinase (PTK2/FAK) is known as the principle kinase involved in anoikis-resistance. FAK activation regulates the turnover of focal adhesions [3] and is caused through the release of autoinhibition of the kinase domain by the FERM domain of FAK [4]. While mechanisms of FAK activation downstream of integrin engagement in focal adhesions have been extensively investigated [5, 6], the mechanism of FAK activation to oppose

anoikis in detached cells has not been investigated.

CDCP1 is a cell surface receptor that sequesters SRC and PKC-δ to plasma membrane subdomains [7]. CDCP1 forms a complex with β1-integrin that is required for tumor metastasis [8]. The shedding of the CDCP1 ectodomain through cleavage by plasmin is another mechanism critical for metastatic dissemination [9, 10]. Reduced CDCP1 expression has been linked to cell detachment and anchorage-independent growth [11-13]. We demonstrated that in the detached state reduced CDCP1 expression abolishes the activity of CDK5, which leads to the loss of inside-out activation of β1-integrin [11]. In patients with lethal, metastatic castration-resistant prostate cancer (mCRPC), reduced CDCP1 was observed in circulating tumor cells (CTCs) and in approximately 50% of mCRPC tissues [11, 14].

The first *in vivo* evidence of the pro-oncogenic phenotype resulting from loss of CDCP1 and its connection to FAK activation emerged from a genetically engineered PyMT mouse model of basal type breast cancer [15]. FAK activation was observed when explanted PyMT CDCP1 knockout cancer cells were detached from extracellular matrix (ECM) and cultured in suspension. Expression of CDCP1 prevented FAK activation in detached cells [16]. However, the mechanism leading to FAK activation downstream of CDCP1-loss remained unclear.

A potential mechanism of direct FAK kinase activation in the detached state and independent of integrin engagement is through PtdIns[4,5]P_2 (PI(4,5)P_2). Structural analysis demonstrates that PI(4,5)P_2 binds to the FERM domain of FAK [4, 17, 18]. The production of PI(4,5)P_2 occurs under tight spatial regulation by phosphatidylinositol 4-phosphate 5-kinases (PIP5K) [19, 20]. The PIP5K1c-v2 (PIP5K1c-201) isoform is associated with focal adhesions and responsible for FAK activation. This PIP5K1c isoform is the only isoform containing Exon17, which puts the PIP5K1c under regulation by the c-SRC kinase [21]. Phosphorylation of PIP5K1c-Y644 by SRC leads to activation of PIP5K1c by inducing Talin binding and the switch of Talin binding from β1-integrin to PIP5K1c [22, 23]. We hypothesized that this mechanism, which is independent of cell adhesion, may be responsible for detachment activation of FAK.

In this study we demonstrate how FAK is activated in CDCP1^{Low} PC cells upon detachment from ECM. Using CTCs from patients with mCRPC, a PC xenograft mouse model and normal human primary lymphocytes, we establish the molecular association between loss of CDCP1 and FAK activation. We demonstrate that FAK activation in the detached state occurs by the convergence of three pathways. We also demonstrate that loss of CDCP1 increases the sensitivity of detached PC cells to FAK inhibitors. Reduced expression of CDCP1 leads to a decline in β1-integrin activation, the loss of CDCP1 may participate in coordinating cell detachment from ECM and FAK activation. This mechanism would be able to overcome anoikis and allow PC cells to survive bottlenecks of tumor metastasis that involve cell detachment, such as vascular intravasation.

Materials and methods

Antibodies

The following antibodies were purchased from Cell Signaling Technologies: Rabbit anti-human CDCP1 (#4115), β1 Integrin (#4706), Phospho-SRC (#2101), SRC (#2108), Phospho-FAK (#8556), Phospho-FAK (#3281), Phospho-FAK (#3284), FAK (#13009), Phospho-p44/42 (ERK1/2) (#4377), p44/42 (ERK1/2) (#9102), Phospho-Akt (Thr308) (D25E6) XP® Rabbit mAb #13038, Akt (#9272), GFP (D5.1) XP® Rabbit mAb #2956, Anti-rabbit IgG, HRP-linked Antibody #7074. Activated β1-integrin (HUTS4, MAB2079Z) was obtained from Millipore (400 Summit Drive, Burlington, MA, 01803).

Pharmalogical inhibitors PF573228 (#PZ0117) and PD98059 (#P215) were purchased from Sigma-Aldrich. Saracatinib (#S1006) was purchased from Selleckchem (9330 Kirby Drive, STE 200, Houston, TX, 77054). All experiments were conducted with three technical and two biological replicates.

Human Plasma (#P9523) and Bovine Serum Albumin (#05470) were purchased from Sigma-Aldrich. Exogenous Phosphatidylinositol 4,5-bisphosphate diC8 (PI(4,5)P_2 diC8) (PI(4,5)P_2) (P-4508-100UG) was purchased from Echelon Biosciences, Inc. FAK plasmid pLV-neo-CD2-FAK (#37013) and PIP5K plasmid GFP-PIPK1-gamma 90 (#22299) were purchased from Addgene. Mutant constructs were generated

with Agilent Technologies QuikChange Site-Directed Mutagenesis Kit (#200518).

Study approval

All experiments were conducted with approval from the institutional review board and the animal welfare committee of Cedars-Sinai Medical Center.

NanoVelcro CTC analysis in a cohort of metastatic PC

Patients provided permission for CTC analysis by signing a consent. CTCs were enriched and captured by the NanoVelcro CTC platform using similar protocols as described in [24]. The NanoVelcro CTC isolation system combines streptavidin-coated three-dimensional nanostructured substrates and an overlaid polydimethylsiloxane microfluidic chaotic mixer to capture CTCs. Venous blood was collected in acid-citrate dextrose-containing vacutainers (BD Bioscience, San Jose, CA, USA) from mCRPC patients under the existing protocols approved by the Cedars-Sinai Medical Center (CSMC) and processed within 24 hours. Following density gradient centrifugation, 1 mL of separated peripheral blood mononuclear cells (PBMC) were incubated with a capture agent (biotinylated anti-human EpCAM antibody, R&D Systems, Minneapolis, MN, USA). The sample was then loaded into the NanoVelcro chip, which contains an automated fluid handler at (0.5 mL/hr). Cells captured on the surface of the chip were fixed with 2% paraformaldehyde (PFA, Electron Microscopy Science) and stained by immunocytochemistry (ICC) with DAPI (Vector Laboratories, Burlingame, CA, USA), mouse anti-pan-cytokeratin (Agilent Technologies, Santa Clara, CA, USA), rat anti-CD45 (Life technologies, Carlsbad, CA, USA), and rabbit anti-FAK-pY379 (Cell Signaling Technology, Danvers, MA, USA). Cells were visualized with Alexa Fluor 488-conjugated anti-mouse (Invitrogen, Carlsbad, CA, USA), Alexa Fluor 555-conjugated anti-rabbit (Invitrogen, Carlsbad, CA, USA), and Alexa-647 donkey anti-rat (Abcam, Cambridge, MA, USA) antibodies.

Imaging of stained CTCs

An automated scan of the NanoVelcro chip was conducted (10X) for enumeration and images of cells were taken at 40X using an upright fluorescence microscope (Eclipse 90i, Nikon) with NIS-Element imaging software (Nikon) for visualization of nuclear and cytoplasmic staining. A multi-wavelength filter cube device permitted the separation of signals from fluorophores with different emission wavelengths (DAPI (nucleus), FITC (CK), CY5 (CD45) and TRITC (FAK-pY379). CTCs displayed positive DAPI and CK staining and were negative for CD45 staining. These cells were selected for quantification of FAK-pY379 expression. FAK-pY379 signal intensity was measured using ImageJ in the CK and/or DAPI positive pixel areas. The average staining intensity in the FAK-pY397 channel was determined and the background was subtracted. The resulting value of FAK-pY397 expression in each CTC is plotted on the Y-axis of the graph shown in **Figure 1C**.

Analysis of CDCP1 mRNA expression in CTCs and bulk tumor

CDCP1 mRNA expression in CTCs was measured on the Nanostring® Encounter platform. Custom designed probes for quantification of individual genes were purchased from Nanostring®. Genes were selected based on expression in PC and lack of expression in blood cells. Expression counts for each gene were normalized as described in [43]. Analysis of CDCP1, ONECUT2 and AR in bulk tumor was performed in a subgroup of PCs that displays the greatest variance in ONECUT2 activity based on expression levels of genes comprising the ONECUT2 cistrome. We previously published three subtypes of PC according to pathway activation signatures [31]. Amongst the three subtypes, subtype 3 (PCS3) exhibits the greatest dynamic range of the ONECUT2 activation signature [26]. Therefore, we performed the analysis of ONECUT2, AR and CDCP1 interactions in the PCS3 subtype.

Analysis of FAK in TCGA and PCTA

Data of gene alterations with the focal adhesion associated protein kinase (PTK2/FAK) gene were obtained from The Cancer Genome Atlas through cBioportal (https://www.cbioportal.org/). The Prostate Cancer Transcriptome Atlas (PCTA) [31] was used for analysis of FAK activity signatures procured from data published [29, 30]. Genes differentially expressed in wild type and $FAK^{-/-}$ murine squamous carci-

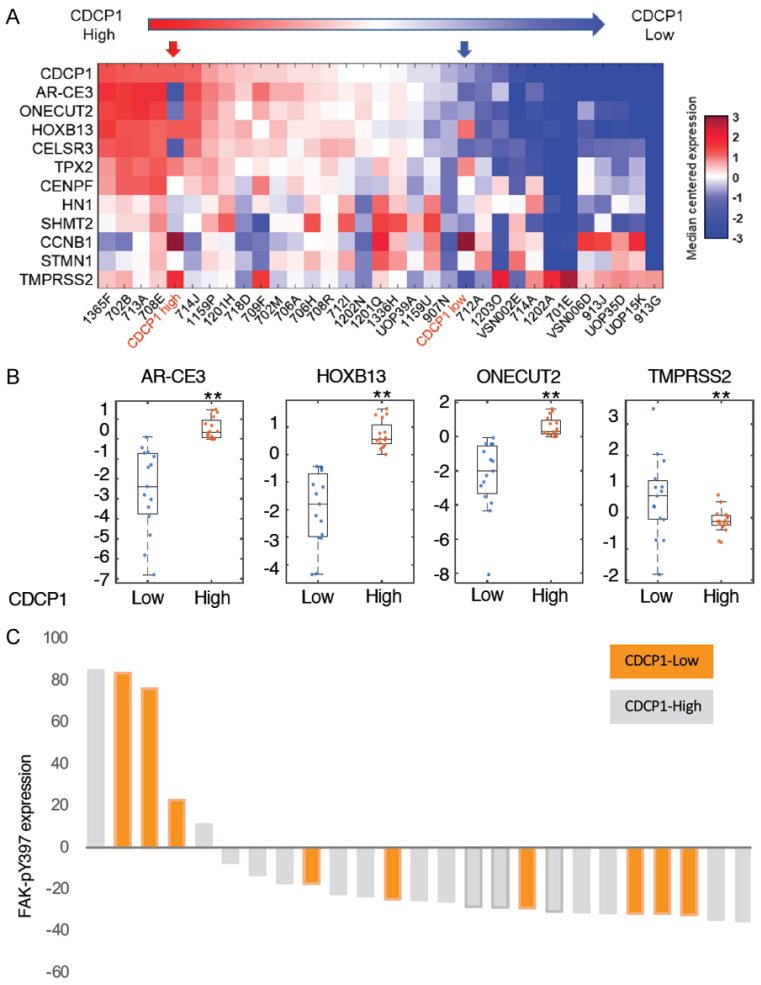

Figure 1. CDCP1 and ONECUT2 subgroups in metastatic castration-resistant prostate cancer (mCRPC). A. mRNA expression of CDCP1, ONECUT2 and 10 mCRPC-related genes in CTCs from 23 patients with mCRPC. Cases are ranked based on CDCP1 expression. The red arrow marks CDCP1^{high} PC3 cells and the blue arrow indicates CDCP1^{Low} PC3 cells. B. Boxplots comparing ARv7-CE3, HOXB13, ONECUT2 and TMPRSS2 gene expression levels in top versus bottom CDCP1 quartiles, **P < 0.001. C. Phospho-FAK-Y379 expression in CTCs from 8 patients with mCRPC. Each bar depicts an individual CTC. The mean, background adjusted immunofluorescent signal intensity of FAK-pY379 in individual CTCs is plotted on the y-axis. CTCs are from CDCP1^{High} (grey bar) and CDCP1^{Low} (orange bar) mCRPC patients and are identified by positive DAPI and pan-cytokeratin and negative CD45 staining (Figure S2).

noma cells (SCC) were identified through profiling on Affymetrix microarrays. Differentially expressed genes were separated into groups of reduced or elevated expression levels. Genes with increased expression in FAK$^{-/-}$ compared to wt-FAK SCC were interpreted as regulated in a repressive mode by FAK (FAK^{DOWN} signature), while RNA expression levels of genes downregulated in FAK$^{-/-}$ (FAK^{UP} signature) were interpreted as being induced by FAK. Using the gene sets as a surrogate to determine FAK activation we evaluated changes during PC progression in PCTA and detected a significant change only with the FAK^{DOWN} gene set. The FAK^{UP} signature did not change significantly (ANOVA P > 0.01) during PC progression.

Cell lines and mouse xenografts

Sublines from DU145 and PC3 cells and silencing of CDCP1 were previously described by our group [32]. Cells were authenticated specifically for this study as DU145 or PC3 cells by short tandem repeat profiling and tested free of mycoplasma contamination (University of Arizona Genetics Core). Mouse studies were conducted under an IACUC approved protocol from Cedars-Sinai Medical Center [11]. Investigators were not blinded to the data.

Cell suspension on HEMA-coated plates, Western Blot protocols, co-immoprecipitations and *MTT assays* are described previously [11].

Exogenous PI(4,5)P_2 treatment

Phosphatidylinositol 4,5-bisphosphate diC8 (PI(4,5)P_2 diC8) (PI(4,5)P_2) (P-4508-100UG) was purchased from Echelon Biosciences, Inc. and administered in micelles formed by addition of 0.1% Triton X-100 (Sigma-Aldrich) at the indicated concentrations. DU145 and PC3 cells were treated for 3 hours while suspended in HEMA coated plates.

Bioinformatics analyses of PIP5K1c

To measure mRNA abundance of the PIP5K1c splice variant that contains Exon 17, RNA-Seq reads were mapped to GRCh37 with Gencode [44] v24lift37 annotation using STAR (v2.5.3)

[45]. The GeneCounts parameter was set to TranscriptomeSAM and the resulting bam file was used as input to the rsem-calculate-expression program (v1.3.0) [46]. RSEM isoforms levels of PIP5K1c splicing isoforms were used to calculate the Spearman correlations between PIP5K1C isoforms. The PIP5K1c-201 Ensemble designation (ENST00000335312.7) corresponds the splicing variant designated as PIP5K1c-v2 in functional studies of the splicing isoform [21]. Copy number alteration (CNA) analysis was used to determine the genomic integrity of the PTEN and TP53 genes using single nucleotide detection (SNP) on the OncoScan platform. CNA calls are from OncoScan FFPE Express 3.0 arrays as previously described [34]. Correlation of CNA loss with RNA expression levels was performed in data from the same cases.

FAK mutant constructs

FAK construct pLV-neo-CD2-FAK (#37013) was purchased from Addgene. pLV-neo-CD2-FAK was mutated to a FERM domain mutant according to [17] and a FAT domain mutant according to [47] using Agilent Technologies QuikChange Site-Directed Mutagenesis Kit (#200518) and transfected via electroporation using a Neon transfection system. 48 hours post-transfection, positive cells were selected by 5 days of G418 treatment.

PIP5K1c mutant constructs

The PIP5K1c construct was purchased from Addgene (75 Sidney Street, Suite 550A Cambridge, MA 02139). PIP5K, GFP-PIPK1 gamma 90 (#22299) was mutated to a D316A dominant negative mutant [21] using Agilent Technologies QuikChange Site-Directed Mutagenesis Kit (#200518) and transfected via electroporation using a Neon transfection system. 48 hours post-transfection, positive cells were selected by 5 days of G418 treatment.

Immunocytochemistry/immunofluorescence of lymphocytes

Peripheral blood lymphocytes from normal donors were suspended in HEMA-coated 60 mM tissue culture plates for 3 h in 10% FBS or 1% BSA. Cells were fixed for 10 min with 3.4% PFA and permeabilized/fixed for 30 min. Cells were spun at 1000 × g for 2 min and re-suspended in 1:1000 primary antibodies in 5% goat serum in PBS for 1 h. Cells were washed with PBS, then incubated with 1:2000 secondary antibodies in 5% goat serum in PBS for 30 min. Cells were washed with PBS, mounted with ProLong Gold Antifade (Life Technologies P36930) and Fisher microscope coverglass (Fisher #12-545-83), allowed to dry overnight, and imaged on a Nikon Eclipse TI inverted fluorescent microscope.

Discussion

Both overexpression and reduced expression of CDCP1 are observed in mCRPC [11, 14, 36, 37]. It has been well established that CDCP1 activates β1-integrin [9], enhances cell adhesion, promotes anchorage independent growth and tumor metastasis [9, 38] and leads to activation of the AKT pathway [8]. In addition to pro-oncogenic activities of CDCP1, there is evidence for a tumor suppressive function [37]. The CDCP1 gene is located at the 3p21.3 region of the genome, which is lost in many cancer types [39]. The CDCP1 deficient PyMT breast cancer model possesses enhanced cancer initiation and growth [15, 40]. Exfoliated cells from these tumors exhibit increased growth factor receptor signaling, reduced adhesion and anchorage dependence.

In the current study, we demonstrate that in detached cells, reduced CDCP1 expression unleashes FAK activation by promoting local generation of $PI(4,5)P_2$ through PIP5K1c. In $CDCP1^{Low}$ DU145 cells, PIP5K1c becomes activated by SRC phosphorylation and recruitment of Talin. An association between active FAK-pY397 and PIP5K1c complex formation is observed in $CDCP1^{Low}$ PC cells and in primary lymphocytes, which are CDCP1 negative. Since reduced CDCP1 expression also inhibits β1-integrin activation, the loss of CDCP1 can potentially coordinate the activation of FAK survival pathways with detachment from the substratum (**Figure 7**).

We confirmed and expanded previous data related to the underlying mechanism of PIP5K1c activation in the detached state. Forced expression of PIP5K1c in HEK293 cells led to the first evidence of a PIP5K1c-SRC-Talin complex under anchorage-independent growth conditions [35]. Our study demonstrates that this mechanism is regulated by CDCP1 and associ-

ated with activation of FAK in the detached state in two PC cell lines and in primary lymphocytes. While SRC is required for activation of PIP5K1c, CDK5 inhibits PIP5K1c through phosphorylation [41]. Reduced expression of CDCP1 in detached cells not only promotes SRC phosphorylation of PIP5K1c, but also of the regulatory subunit of CDK5. This causes inactivation of CDK5 and prevents phosphorylation of PIP5K1c by CDK5, which is inhibitory for PIP5K1c activation [42]. In addition, we demonstrate the activation of PIP5K1c in detached cells required human plasma or FBS, however responsible plasma factor and cell surface receptor are currently unknown.

In addition to regulation of FAK, CDK5 and PIP5K1c kinase activities by CDCP1, we identified gene expression differences of targetable transcription factors in CDCP1^{Low} versus CDCP1^{High} CTCs from patients. The expression of CDCP1 mRNA correlates with expression of ONECUT2, a transcription factor that promotes cell survival, castration resistance and neuroendocrine differentiation and that can be targeted by a chemical compound [26]. Another interesting association that is observed only in CTCs and not in bulk tumors lies between CDCP1, AR-v7 and HOXB13 mRNA expression levels. As is the case for ONECUT2, AR-v7 and HOXB13 alter the AR cistrome and cause resistance to AR signaling inhibitors. Thus, in CDCP1^{High} CTCs, ONECUT2 and CDK5 are possible therapeutic targets, while in CDCP1^{Low} CTCs, FAK may be an actionable drug target.

Altogether, CDCP1 regulated cytoplasmic kinase networks and associated gene expression provides a starting point for novel treatment approaches to combat mCRPC.

Results

FAK-pY397 is expressed in CDCP1^{low} circulating tumor cells (CTCs) from patients with metastatic, castration-resistant prostate cancer (mCRPC)

In patients, approximately 50% of metastatic and castration resistant PCs (mCRPC) express high CDCP1, while 50% of mCRPC express reduced levels of CDCP1 protein [14]. CDCP1 has emerged as a new treatment target in mCRPC with PTEN deletion, but the strategy only applies to CDCP1^{High} mCRPC cases [14]. Druggable pathways in CDCP1^{Low} mCRPC have not been elucidated. To explore potentially druggable and pro-metastatic mechanisms in CDCP1^{Low} PC, we investigated the CDCP1-FAK pathway and the cytotoxic effects of FAK inhibition in non-adherent PC cells.

Circulating tumor cells (CTC) from patients with mCRPC were used as a source of non-adherent, detached cancer cells. CTCs were isolated from 31 blood samples of 23 patients using the Nanovelcro system [24] for measurement of mRNA expression. The Nanovelcro platform leads to a large enrichment of CTCs over white blood cells. Since blood lymphocytes and monocytes express negligible amounts of CDCP1 [25], the CDCP1 mRNA signal in our CTC preparation is primarily derived from cancer cells. Each sample provided multiple CTCs that were pooled for RNA extraction. We measured a hand-curated panel of genes associated with aggressive PC that included CDCP1 on the Nanostring® platform. In concordance with published data [11, 14], we observed subgroups of CTCs with high versus low CDCP1 expression (**Figure 1A**). The cut-off between CDCP1^{high} and CDCP1^{Low} CTCs is based on the midpoint of the mean-centered CDCP1 expression. The Nanostring® panel was also used for analysis of mRNA from PC-3 and DU145 cell lines in which we silenced CDCP1 by expression of a CDCP1 shRNA (cell line validation in [11]). A supervised cluster analysis based on CDCP1 expression demonstrated that the CDCP1-knockdown cell lines (**Figure 1A**, blue arrow) co-clustered with CDCP1^{Low} CTCs while the control knockdown cell lines (**Figure 1A**, red arrow) co-clustered with CDCP1^{High} CTCs.

Next, we identified eleven genes that correlated with CDCP1 expression with a correlation coefficient, $r > 0.3$ and a p-value, $P < 0.01$ (**Figure 1A**). These include the *AR-V7* splice variant *(AR-CE3), HOXB13, ONECUT2, CELSR3, TPX2*, and *CENPF.* These genes are known for their association with aggressive PC and are directly regulated by the androgen receptor (AR) [26]. While mRNA expression of *AR-V7, HOXB13* and *ONECUT2* is significantly increased in CDCP1^{high} CTCs ($P < 0.01$), expression of TMPRSS2 is significantly decreased ($P < 0.01$) (**Figure 1B**). We previously demonstrated how ONECUT2 represses the AR axis at multiple levels [26]. Since a recent study demon-

strated that the AR-axis inhibits *CDCP1* gene expression [14, 27], we postulated that the suppression of the AR by ONECUT2 leads to increased CDCP1. To test this premise, we examined the relationship between CDCP1 and ONECUT2 activity (i.e. the z-score of the ONECUT2 cistrome) in bulk tumor tissue. As expected, we observed a positive correlation between CDCP1 gene expression and ONECUT2 activity (Spearman's rho = 0.41, P = 4×10^{-4}) and a negative correlation between CDCP1 and ONECUT2 or AR transcription factor activities (Figure S1).

Next, we interrogated FAK activation in $CDCP1^{High}$ and $CDCP1^{Low}$ CTC populations of patients with mCRPC. We utilized cryopreserved CTCs from patients previously analyzed for CDCP1 mRNA expression (**Figure 1A**). While CDCP1 mRNA was measured in pooled CTCs from each case, FAK activation was measured through expression of FAK-pY397 in individual CTCs using fluorescent in-situ detection with the FAK-pY397 antibody. CTCs from three patients in the $CDCP1^{High}$ and five patients in the $CDCP1^{Low}$ groups were retrieved for analysis. Cases in the $CDCP1^{High}$ group contained 4-7 CTCs for analysis, while $CDCP1^{Low}$ cases only harbored 0-3 CTCs. Therefore, to analyze a comparable number of CTCs in both groups required more $CDCP1^{Low}$ than $CDCP1^{High}$ cases. CTCs were identified through positive cytokeratin and DAP1 and negative CD45 fluorescent staining and FAK-pY397 expression quantified in CTCs using a forth antibody-fluorophore label (Figure S2). In the $CDCP1^{Low}$ group 3/5 (60%) patients demonstrated high FAK-pY397 expression in at least one CTC, while in the $CDCP1^{High}$ group, 1/3 (33%) patients expressed high FAK-pY397 (**Figure 1C**). Because of antibody and imaging limitations, double staining for CDCP1 and FAK-pY397 was not feasible. Therefore, it is uncertain whether intra-patient variability of FAK-pY397 is related to heterogeneous CDCP1 expression across individual CTCs. A statistical analysis of FAK-pY397 data did not reveal a significant difference in FAK-pY397 expression between $CDCP1^{High}$ and $CDCP1^{Low}$ groups because of the low sample size. Nevertheless, there appears to be a trend between the association of reduced CDCP1 expression and FAK activation in the detached state.

To determine the association between FAK activity and PC aggressiveness and progression, we investigated FAK in bulk patient tumors. Gene amplification can result in kinase activation [5]. The FAK gene resides at 8q24.3 and is amplified in 6% of prostate adenocarcinomas and 38% of neuroendocrine PC (**Figure 2A**). In addition to its role in focal adhesion turnover [28], FAK can translocate into the nucleus to regulate gene expression [29]. Both, up (FAK^{UP}) and down (FAK^{DOWN}) regulated FAK-driven gene signatures have been identified in squamous cell carcinoma cell lines [30]. FAK activation signatures were analyzed in the Prostate Cancer Transcriptome Atlas (PCTA, n = 1352) [31], which is a cohort of cases that spans the entire PC disease course from benign prostate tissue to metastatic and castration-resistant PC. While the signature of genes positively regulated by FAK did not show a significant change during PC progression (Figure S3), the signature of genes that are suppressed by FAK revealed a remarkable decline along the PC disease course (**Figure 2B**). The consistent decline of the FAK^{DOWN} gene signature with increasing cancer grade and stage is suggestive of an increase in FAK activity during PC progression.

$CDCP1^{low}$ PC xenografts express activated FAK despite inactive β1-integrin

To investigate how FAK is activated in $CDCP1^{Low}$ PC cells, we employed cell culture models of DU145 and PC-3 that we published previously [32]. In cells derived from these models, reduced expression of CDCP1 stimulates DU145 xenograft growth (**Figure 2C** and [11]). We generated five xenografts from the $CDCP1^{Low}$ cell populations that were established by transfection of shCDCP1 without further clonal selection. As a result of heterogeneous CDCP1 expression in the inoculated cells, four of five xenografts did not express CDCP1, while one xenograft was CDCP1 positive (**Figure 2C**). FAK-pY397 expression was increased in the four $CDCP1^{Low}$ xenografts compared to $CDCP1^{High}$ xenograft. Interestingly, three of four xenografts with active FAK-pY397 expression revealed greatly diminished active β1-integrin as measured by the HUTS4 antibody which is specific for the active state of β1-integrin. These data are consistent with our previous study showing that β1-integrin is inactivated after silencing of CDCP1 and demonstrate that FAK activation can occur in cancers with inactive β1-Integrin. To determine whether reduced CDCP1 expression promotes

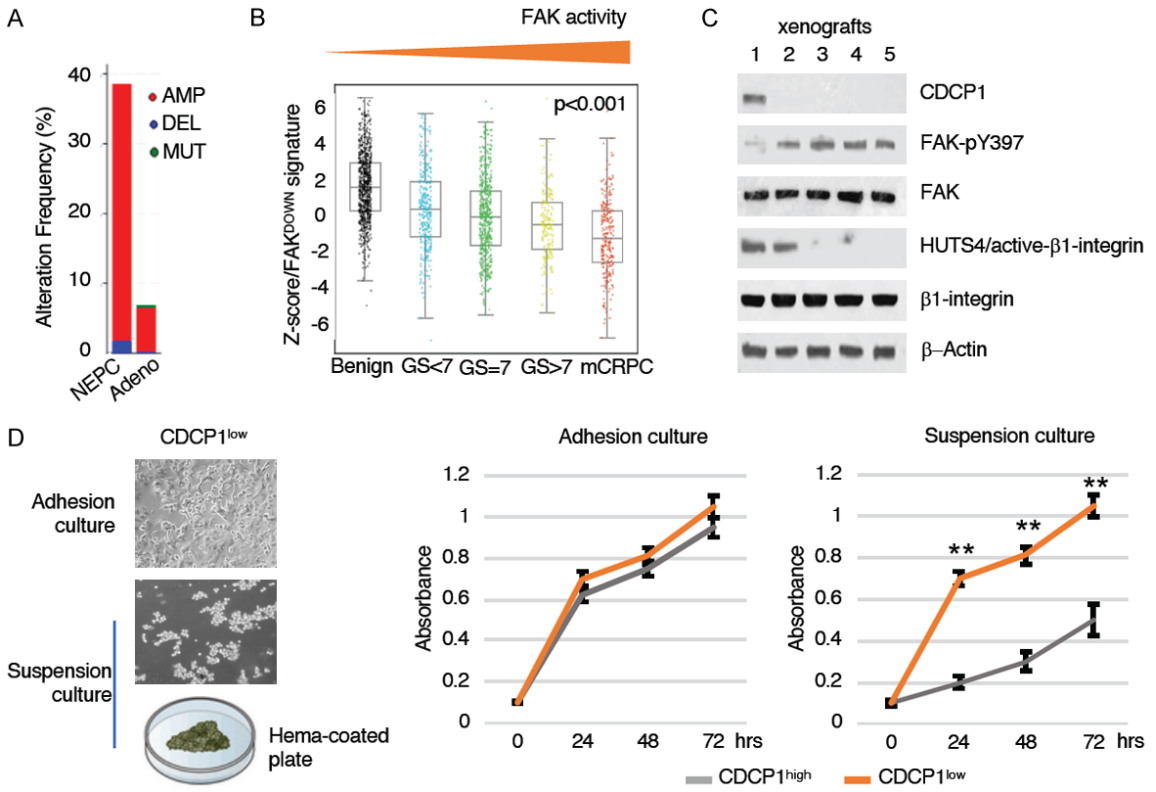

Figure 2. FAK activation in prostate cancer cells. A. *FAK* gene amplifications (AMP), deletions (DEL) or mutations (MUT) in neuroendocrine PC (NEPC, n = 114) or prostate adenocarcinoma (TCGA, n = 494). B. A FAK-repressed gene signature increases with PC progression. A panel of FAK-repressed genes (Table S1) is analyzed in the Prostate Cancer Transcriptome Atlas (PCTA, n = 1352 [31]). The z-scores of the FAK signature in cases of benign prostate, low grade (Gleason Sum < 7), intermediate grade (Gleason Sum = 7), high grade (Gleason Sum > 7) and metastatic castration-resistant PC (mCRPC) are shown. The *p*-value is from the ANOVA test of z-scores of the FAK-repressed gene signature. C. Xenograft analysis of CDCP1^{Low} DU145 cell line xenografts. Whole cell lysates from xenografts were analyzed by Western blotting for expression of FAK-pY397 and activation state of β1-integrin. The HUTS4 antibody binds selectively to the active configuration of β1-integrin. D. CDCP1 loss promotes survival in the detached state. Images of adherent (upper panel) and detached (lower panel) CDCP1^{low} cultures. At indicated time points, cells were stained with Trypan blue and viable cells were counted. Growth curves of adherent and detached cultures. Absorbance data from MTT assays [31]. **P < 0.01.

tumor cell growth in the detached state, we employed a suspension culture system (**Figure 2D**). Growth curves of CDCP1^{High} and CDCP1^{Low} DU145 cells were identical in adherent culture, but differed significantly in suspension culture (**Figure 2D** right panel). The main difference between CDCP1^{High} and CDCP1^{Low} PC cells was observed during the first 24 hours in suspension culture, consistent with a pro-survival effect of reduced CDCP1 expression. After 24 hours in culture, those CDCP1^{High} cells that survived, proliferated at a rate similar to CDCP1^{Low} cells, as indicated by the parallel growth curves. Since FAK activation is known to stimulate cell survival in the detached state, we hypothesized that FAK activity in CDCP1^{Low} cells is the reason for the increased survival of CDCP1^{Low} PC cells.

Low CDCP1 sensitizes detached PC cells to killing by FAK inhibitors

To further pursue the mechanism underlying the potential inverse relationship of FAK and β1-integrin activation in cell line xenografts, we analyzed adhesion and suspension cultures of DU145 and PC3 cells (**Figure 3**). CDCP1^{High} and CDCP1^{Low} DU145 and PC3 cells were compared for expression of FAK-pY397 and HUTS4 (**Figure 3A**). Cells were suspended for 2 hours in media containing 10% FBS. In addition to phosphorylation of FAK-Y397, we observed phosphorylation of FAK-Y576/577 and FAK-Y925, which are SRC phosphorylation sites in the FAK protein. We did not examine the FAK-Y861 phosphorylation site, since its regulation by CDCP1 has been previously ana-

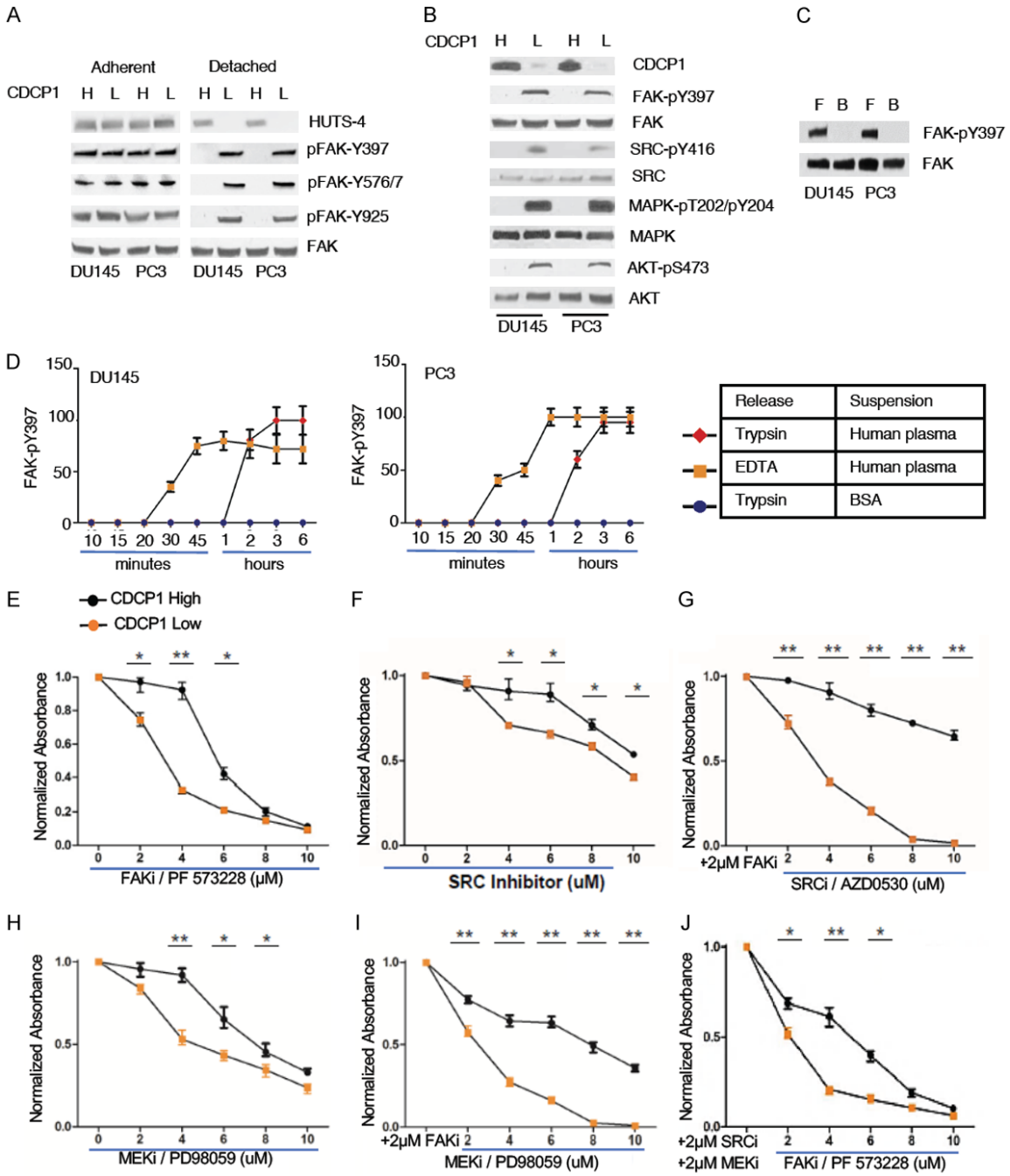

Figure 3. CDCP1 loss sensitizes DU145 PC cells to FAK Inhibitor treatment. A. Suspension-activation of FAK. Cell lysates from CDCP1^{Low} and CDCP1^{High} DU145 and PC3 cells were probed with anti-FAK-pY379 (FAK autophosphorylation site), anti-FAK-pY576/7 (SRC phosphorylation site) and anti-FAK-pY925 (SRC phosphorylation site). B. Detached CDCP1^{Low} or CDCP1^{High} PC cells were probed for active, phosphorylated FAK, SRC, MAPK and AKT and reprobed for total protein expression. C. FAK activation requires fetal bovine serum (FBS). Cells were cultured in suspension with 10% FBS (F) or 1% bovine serum albumin (BSA, B). Western blots were probed for FAK-pY397 and reprobed for total FAK. D. FAK activation by human plasma. CDCP1^{Low} DU145 and PC3 PC cells were cultured under detached conditions in 10% human plasma (squares) or BSA (circles) containing media for times indicated and probed for expression of FAK-pY397. Cells were released from culture dishes with either trypsin (red) or EDTA (yellow). The y-axis represents the relative amount of FAK-pY397 expression based on quantification of Western Blot bands in Figure S3. E, F and H. Growth inhibition of DU145 cells treated with single drug treatments of FAK inhibitor, PF573228, SRC inhibitor, AZD0530 (Saracatinib) or MEK inhibitor (PD98059) at concentrations indicated on the x-axis. Cells were preincubated with drugs before release from culture plates and drug treatments were continued in suspen-

sion for 24 hours. G, I and J. Growth inhibition of DU145 cells treated with drug combinations. DU145 cells were treated with 2 uM PF 573228 (FAK inhibitor) plus AZD0530 (Saracatinib, SRC inhibitor), PD98059 (MEK inhibitor) or AZD0530 and PD98059. X-axis labels indicate drug concentrations and Y-axis labels the percentages of viable cells. *P < 0.05, **P < 0.01.

lyzed [33]. In addition to FAK activation, SRC, MAPK and AKT activities were increased in detached CDCP1^{Low} compared to CDCP1^{High} PC cells (**Figure 3B**). To determine whether extracellular factors are required for FAK activation, we tested human plasma as a source of factors for FAK activation in CTCs and primary human lymphocytes and fetal bovine serum (FBS) as a source of factors in detached cell cultures. In addition, we tested the sensitivity of FAK activation to trypsinization conditions. Cells were released from culture plates using either trypsin or EDTA. After a washing step, cells were suspended in media containing 10% human plasma, 10% FBS or 1% BSA. The cells were kept in a detached and floating state without adhesion to plastic on HEMA coated plates for the duration of the experiment. FAK-pY397 expression in DU145 and PC3 cells required FBS or human plasma (**Figure 3C**, **3D**). Surprisingly, FAK phosphorylation was only observed after 2 hours in suspension after detachment by trypsin (Figure S4). In contrast, when cells were released from plastic dishes with EDTA, FAK phosphorylation occurred after 30 minutes (**Figure 3D**). FAK was not activated by treatment with a preparation of exosomes that were isolated from the serum-free conditioned medium of CDCP1^{Low} cells (Figure S5). Altogether, these data demonstrate that FAK activation in CDCP1^{Low} cells requires human plasma or FCS and a trypsin sensitive cell surface receptor.

Next, we questioned whether detached cells with increased FAK activation are more sensitive to FAK inhibitors. Cells were treated with FAK, SRC and MEK inhibitors and drug effects confirmed by Western blotting (Figure S6). We observed that loss of CDCP1 sensitized cells to FAK inhibitors. The GI50 for the FAK inhibitor, PF573228, in CDCP1^{low} cells was 3 uM compared to 6 uM in CDCP1^{high} cells. The greatest difference in cytotoxicity was observed reproducibly at the 4 uM concentration (**Figure 3E**). Adding the SRC inhibitor, Saracatinib, or a MEK inhibitor to 2 uM FAK inhibitor demonstrated an additive effect (**Figure 3F-I**). The combination of 3 drugs revealed lower cytotoxic concentrations of individual compounds, suggestive of an additive effect (**Figure 3J**). In contrast to the FAK kinase inhibitor, an inhibitor directed against the FAT domain of FAK or the expression of a FAT-domain mutant FAK did not demonstrate reduced FAK-pY397 expression in the detached state of CDCP1^{Low} DU145 cells (Figure S7). These results provide pre-clinical evidence that FAK inhibitors might be more effective in PC cells with low CDCP1 expression.

Detached, CDCP1^{low} PC cells activate FAK independent of β1-integrin

We previously demonstrated that CDCP1 maintains β1-integrin in an active configuration after cell detachment through CDK5-mediated phosphorylation of Talin and that reduced CDCP1 leads to loss of inside-out activation of β1-integrin [11]. Since FAK is activated downstream of β1-integrin in adherent cells, we questioned whether active CDK5/β1-integrin was a requirement for FAK activation in detached, non-adherent cells and controlled the activation state of β1-integrin in the detached state through silencing of CDCP1. Lysates from CDCP1^{Low} and CDCP1^{High} cells were used in co-immunoprecipitation experiments to examine β1-integrin and CDK5 complex formation with FAK. As expected, β1-integrin in detached CDCP1^{High} PC cells is complexed to pTalin/CDK5/CDKR1, which maintains the inside-out activation of β1-integrin (**Figure 4A**, green box). However, surprisingly, despite β1-integrin activaion, FAK kinase is inactive in the β1-integrin complex. In contrast, in detached CDCP1^{Low} DU145 cells, FAK is active while β1-integrin is inactive (**Figure 4A**). In addition, reduced CDCP1 expression in the detached state leads to dissociation of CDK5 from the β1-integrin complex. CDK5 in detached CDCP1^{Low} cells is inactive and exists in a complex with active FAK-pY397. Thus FAK-pY397 resides in two separate complexes, one with β1-integrin and the other with CDK5 (**Figure 4A**, **4B**). Interestingly, Talin-pS425, which is found in the β1-integrin complex in CDCP1^{High} cells, moves into the CDK5 complex in CDCP1^{Low} cells (**Figure 4A**, **4B**).

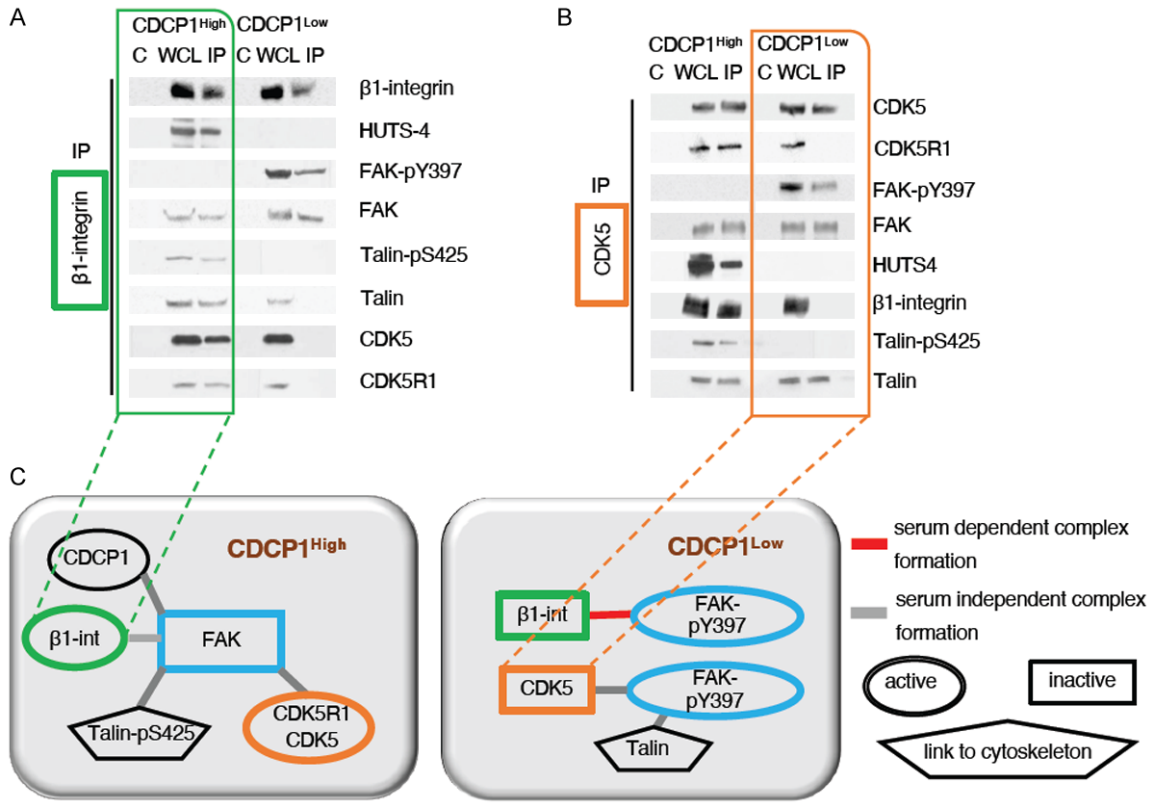

Figure 4. FAK protein complexes are regulated by CDCP1 in the detached state. Comparison of protein complexes in detached CDCP1^{High} and CDCP1^{Low} DU145 cells. Protein lysates from CDCP1^{High} and CDCP1^{Low} DU145 cells were divided into two equal parts for analysis of either β1-integrin complexes or CDK5 complexes by co-precipitation. A. β1-integrin/Talin/FAK complex. β1-integrin was precipitated and the protein complex was probed for FAK-pY397/total FAK, Talin-pS425/Talin, CDK5 and CDK5R1. B. CDK5/FAK complex. CDK5 was precipitated and the complex probed for FAK-pY397/FAK, HUTS4 (active β1-integrin)/total β1-integrin and Talin-pS425/Talin. C. Schematic illustration of FAK complexes in CDCP1^{High} versus FAK-pY397 in CDCP1^{Low} cells. The serum dependence of complex formation is indicated by the color of the bar. C-control antibody precipitation, WCL-whole cell lysate, IP-immunoprecipitation.

Since FAK activation requires FBS, we analyzed the regulation of FAK complexes by FBS. Complex formation of inactive β1-integrin with active FAK-pY397 requires FBS, while FAK-CDK5 complexes form without FBS (Figure S8). A summary of regulation of FAK complexes by CDCP1 is shown in **Figure 4C**. Together the data support a model in which reduced expression of CDCP1 in the detached state leads to β1-integrin-independent FAK activation.

In the detached state, FAK is activated by PI(4,5)P$_2$

Since FAK activation (i.e. expression of FAK-pY397) in detached CDCP1^{Low} PC cells occurs in the absence of active β1-integrin, we examined alternative mechanisms of FAK activation. One mechanism of FAK activation is through the binding of PI(4,5)P$_2$ to the FERM domain (**Figure 5A**). To demonstrate that FAK can be activated by PI(4,5)P$_2$ in the detached state, we treated suspended cells with exogenous PI(4,5)P$_2$. PI(4,5)P$_2$ activation of FAK was concentration dependent and did not require FBS (**Figure 5B**, 1% BSA condition). Furthermore, exogenous treatment with PI(4,5)P$_2$ resulted in FAK-pY397 in CDCP1^{High} cells, demonstrating that PI(4,5)P$_2$ reverses the upstream inhibition of FAK activation by CDCP1 (**Figure 5B**).

In the detached state, reduced CDCP1 activates PIP5K1c/PI(4,5)P$_2$ through SRC phosphorylation and Talin binding

PI(4,5)P$_2$ is produced by three PIP5K isoforms that differ in subcellular localization. Only the PIP5K1c-201 isoform is associated with cell adhesion complexes. PIP5K1c-201 differs from other isoforms by the inclusion of

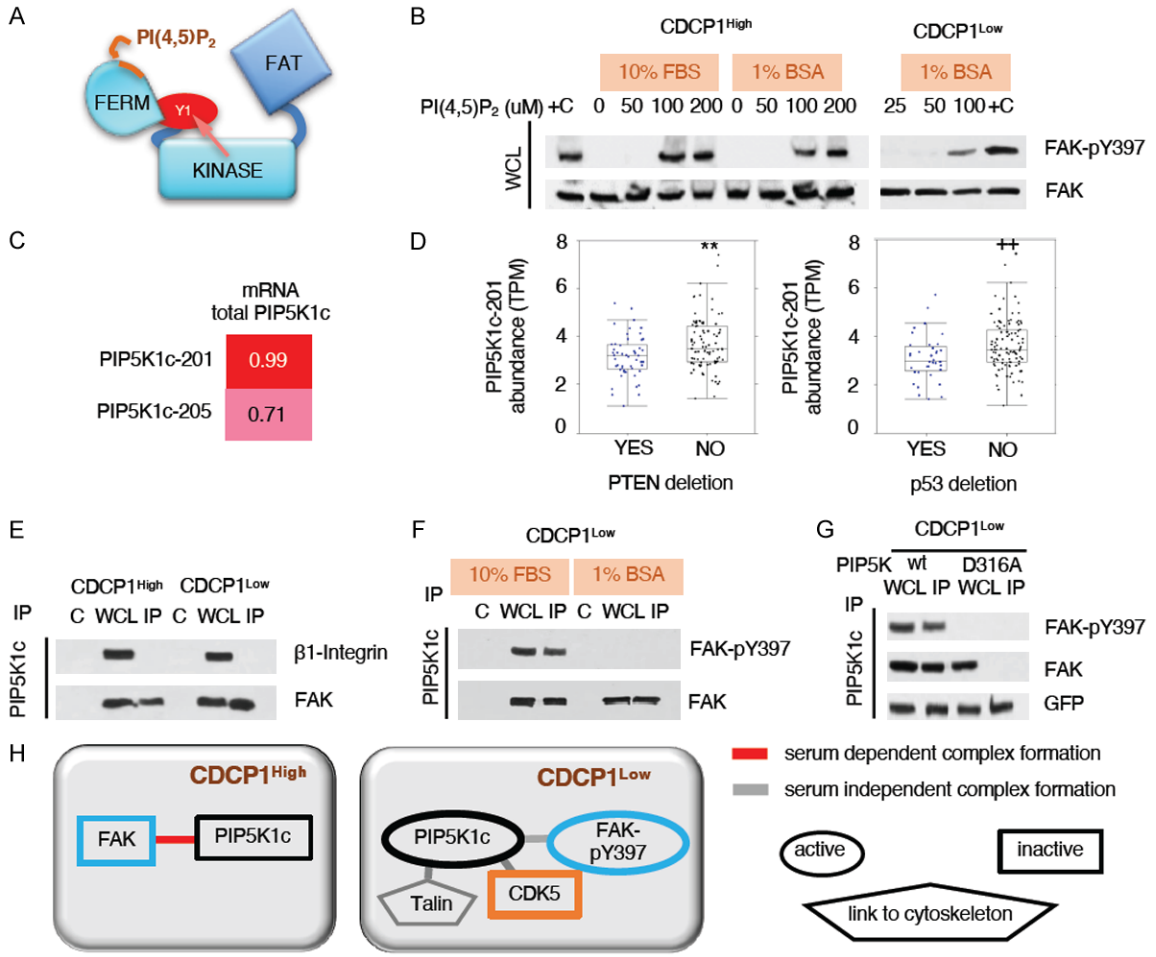

Figure 5. Suspension-activation of FAK by *PtdIns*(4,5)P_2 (PI(4,5)P_2). A. Binding to PI(4,5)P_2 releases the autoinhibition of the FERM domain. Activation of the FAK kinase results in FAK-pY397 (Y1) expression. B. Exogenous PI(4,5)P_2 activates FAK. Detached CDCP1^{High} DU145 cells, which remain FAK-pY397 negative in 10% FCS or 1% BSA were treated for 3 hours with PI(4,5)P_2 at concentrations specified above each column. Western blots were probed for FAK-pY397 expression. Detached CDCP1^{Low} DU145 cells (FAK-pY397 negative) were cultured in 1% BSA and treated with PI(4,5)P_2 at concentrations specified above each column. Western blots were probed for FAK-pY397 expression. C. Expression of PIP5K1c splicing isoforms. Spearman correlation coefficients between total PIP5K1c mRNA expression and expression of PIP5K1c-201 (Exon 17 positive) and PIP5K1c-205 (Exon 17 negative) splicing isoforms in intermediate risk PC (n = 144, [34]). D. Association of PIP5K1c-201 with PTEN and TP53 loss. Expression levels of PIP5K1c-201 mRNA, indicated as TPM (transcripts per million) are compared in cases with an intact PTEN or TP53 gene locus versus cases with PTEN or TP53 bi-allelic deletions. Deletions were detected by the Oncoscan SNP-chip arrays. Box and whisker plots with horizontal lines in boxes representing the 1st, 2nd and 3rd quartiles. Whiskers are indicated outside the box with limits of 1.53 of the interquartile range. **p = 2.36 X 10^{-3}; ++p = 8.18 X 10^{-3}. E. PIP5K1c-FAK complexes lack β1-integrin. PIP5K1c was precipitated from detached CDCP1^{High} and CDCP1^{Low} DU145 cells and probed for β1-integrin and FAK. F. Serum dependence of FAK-PIP5K1c complexes. G. PIP5K1c-D316A mutant. A GFP-fusion protein of a kinase-dead mutant PIP5K1c or of wild type PIP5K1c was expressed in detached CDCP1^{Low} DU145 cells. Cells were cultured in the detached state with 10% FCS for 3 hours before precipitation of PIP5K1c. Immunoprecipitated complexes were analyzed for FAK-pY397 and FAK. C-control antibody precipitation, WCL-whole cell lysate, IP-immunoprecipitation. H. Schematic representation of PIP5K1c-FAK complexes in CDCP1^{High} versus CDCP1^{Low} PC cells. Talin-PIP5K1c complexes are shown in detail in **Figure 6**.

Exon 17, which contains a unique SRC phosphorylation site [22]. Analysis of cases from a cohort of intermediate risk PC patients [34] revealed that PIP5K1c-201 strongly correlates with total PIP5K1c mRNA expression *(r = 0.99)* (**Figure 5C**). Further, PIP5K1c-201 was significantly reduced in tumors with *PTEN* and *TP53* gene deletions, which are genetic alterations associated with aggressive PC behavior (**Figure 5D**).

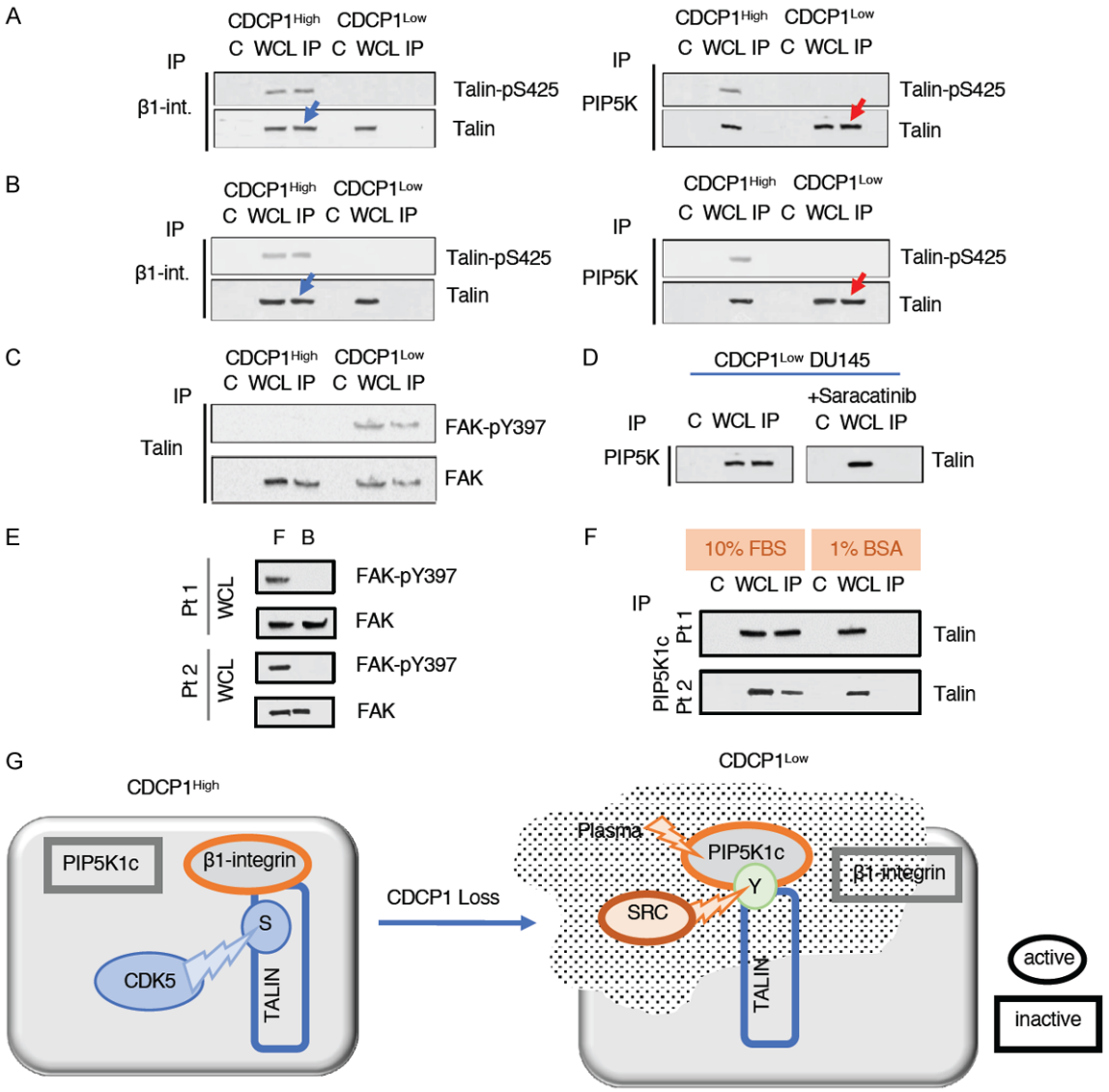

Figure 6. Suspension-activation of PIP5K1c through a Talin switch. A. β1-integrin and PIP5K1c co-immunoprecipitation with Talin. CDCP1^{High} and CDCP1^{Low} DU145 and PC3 cells were used for precipitation of β1-integrin or PIP5K1c. Western blots of protein complexes were probed for Talin-pS425 and total Talin. The blue arrow points to Talin in complex with β1-integrin in CDCP1^{High} cells, while the red arrow points to Talin complexed to PIP5K1c in CDCP1^{Low} cells. B. Talin complexes in mouse xenografts. Co-immunoprecipitation of PIP5K1c and β1-integrin in CDCP1^{High} or CDCP1^{Low} DU145 xenografts. Xenografts #1 (CDCP1^{High}) and #4 (CDCP1^{Low}) described in **Figure 2C** were used. The blue arrow points to Talin in complex with β1-integrin, while the red arrow points to Talin complexed to PIP5K1c. C. FAK-pY397-Talin complexes in CDCP1^{Low} DU145 cells. D. PIP5K1c-Talin complex formation requires SRC phosphorylation. PIP5K1c was immunoprecipitated from detached CDCP1^{Low} DU145 cells treated with 10 uM Saracatinib or control vehicle for 48 hours. Immunoprecipitates were probed for Talin. E. Primary, lymphocytes from 2 separate individuals were cultured in 10% FBS (F) or 1% BSA (B) and analyzed for expression of FAK-pY397 and total FAK protein by Western blotting. F. The same lymphocyte lysates were used for immunoprecipitation of PIP5K1c. PIP5K1c complexes were probed for expression of Talin-pS425 and total Talin. C-control antibody precipitation, WCL-whole cell lysate, IP-immunoprecipitation. G. Schematic illustration of Talin complexes in CDCP1^{High} versus CDCP1^{Low} PC cells.

To determine whether FAK activation through PIP5K1c is regulated by complex formation in detached CDCP1^{Low} PC cells, we immunoprecipitated PIP5K1c and probed for FAK and β1-integrin (**Figure 5E**). Although we observed the formation of PIP5K1c-FAK-pY397 complexes, β1-integrin was not part of these complexes. Further, the formation of PIP5K1c-with inac-

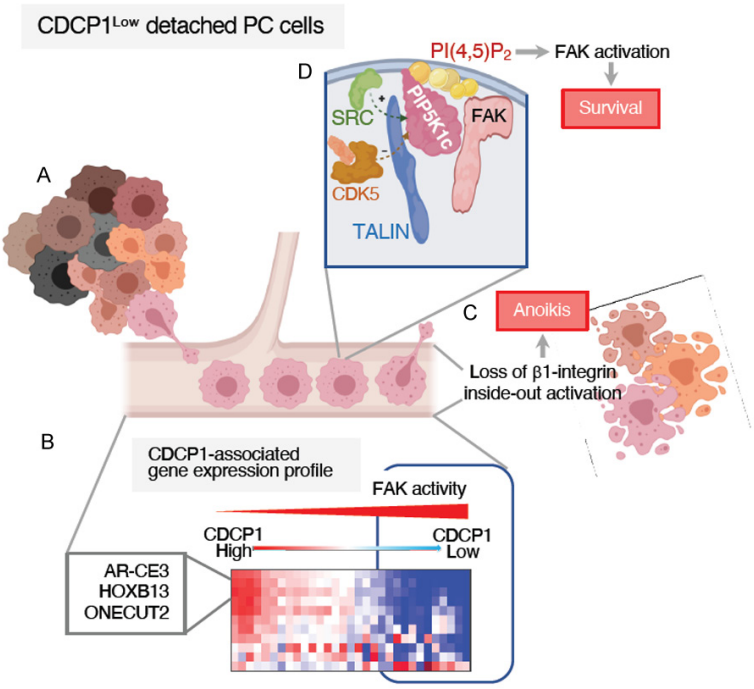

Figure 7. Loss of CDCP1 coordinates cell detachment and survival. (A) Loss of CDCP1 (pink color) can occur through TGFβ1 [11], promoter methylation [48] or palmitoylation [49] and (B) is associtated with an altered gene expression program in the detached state and an increase in FAK activation. (C) Normally, loss of adhesion rapidly results in anoikis. (D) To overcome anoikis, FAK is activated through localized production of $PI(4,5)P_2$ by PIP5K1c. PIP5K1c activation requires SRC phosphorylation and Talin binding and is negatively regulated by CDK5 phsophorylation. By coordinating cell detachment and FAK activation, the loss of CDCP1 facilitates cell survival during tumor metastasis.

tive FAK in $CDCP1^{Low}$ PC cells occurred spontaneously without a requirement for FBS, but FAK activation (i.e. FAK-pY397) requires FBS (**Figure 5F**). To determine the role of $PI(4,5)P_2$ for FAK activation in detached cells, we expressed a kinase-dead PIP5K1c, PIP5K1c-D316A. PIP5K1c-D316A blocked the activation of FAK in a dominant negative manner by competing with wild type PIP5K1c for binding to FAK (**Figure 5G**). In summary, in the detached state, reduced expression of CDCP1 leads to PIP5K1c activation, local production of $PI(4,5)P_2$, changes of FAK protein complexes and activation of FAK (**Figure 5H**).

Next we investigated the mechanism leading to PIP5K1c activation in the detached state. PIP5K1c has previously been demonstrated to reside in a complex with SRC and Talin under anchorage independent growth conditions. Under these conditions, PIP5K1c requires SRC phosphorylation and Talin binding for activation [35]. To determine whether reduced expression of CDCP1 in the detached state leads to formation of Talin-PIP5K1c complexes, we compared Talin-PIP5K1c and Talin-β1-integrin complexes in $CDCP1^{High}$ and $CDCP1^{Low}$ cells. We precipitated β1-integrin from lysates of detached $CDCP1^{High}$ DU145 cells and PIP5K1c from lysates of detached $CDCP1^{Low}$ DU145 cells. As expected in detached $CDCP1^{High}$ PC cells, Talin forms a complex with the active β1-integrin (**Figure 6A** blue arrow). However, upon reduced expression of CDCP1 ($CDCP1^{Low}$ columns in **Figure 6A**), Talin no longer interacts with active β1-integrin. Instead, Talin forms a complex with PIP5K1c in $CDCP1^{Low}$ but not in $CDCP1^{High}$ cells (**Figure 6A**, red arrow). This complex formation requires 10% FBS (Figure S9). The switch of Talin from β1-integrin to PIP5K1c was also observed in $CDCP1^{Low}$ xenografts (**Figure 6B**). Furthermore, in $CDCP1^{Low}$ xenografts, FAK-pY397 is associated with Talin-PIP5K1c complexes (**Figure 6C**). Next, we determined whether SRC activity is needed for formation of Talin-PIP5K1c complexes in detached $CDCP1^{Low}$ PC cells. PC cells were treated with 10 uM Saracatinib, a specific SRC kinase inhibitor during culture in suspension. Treatment with Saracatinib abolished Talin-PIP5K1c complexes (**Figure 6D**).

To demonstrate the association between FAK activation (i.e. FAK-pY397 expression) and Talin-PIP5K1c complexes in a different system, we analyzed primary lymphocytes. Lymphocytes are naturally non-adherent and CDCP1 negative. Lymphocytes from two separate individuals were cultured in 10% FCS or 1% BSA and analyzed for expression of FAK-pY397 (**Figure 6E**). The same lysates were analyzed for PIP5K1c-Talin complexes by immunoprecipitation. Western blotting confirmed that 10% FCS induces FAK-pY397 and leads to formation of PIP5K1c-Talin complexes (**Figure 6F**), while culture in BSA does not. In summary,

when cells are maintained in a detached state, SRC phosphorylates PIP5K1c, which causes the switch of Talin from β1-integrin to activate PIP5K1c (**Figure 6G**). In these cells, activation of PIP5K1c is associated with expression of FAK-pY397.

Acknowledgements

This manuscript is dedicated to Dr. Leland Chung and to his lifelong creative and passionate pursuit of cancer research that provided many concepts and tools for developments of individualized patient care. We thank Dr. Adam Byron for helpful discussions. This work was supported by Department of Defense Synergistic Idea Development Award W81XWH-08-1-0268 (BSK), Stephen Spielberg Team Science Award (BSK, MRF); NIH/NCI P01 CA098912-09 (BSK, MRF); NIH R01CA131255 (BSK); PCF Challenge Award 2017 (BSK) and start-up funding from Cedars-Sinai Medical Center.

Disclosure of conflict of interest

None.

Address correspondence to: Beatrice S Knudsen, Department of Pathology, University of Utah, 2000 Circle of Hope Rm.3100, Salt Lake City, UT 84112, USA. E-mail: Beatrice.Knudsen@path.utah.edu

References

[1] Frisch SM and Francis H. Disruption of epithelial cell-matrix interactions induces apoptosis. J Cell Biol 1994; 124: 619-626.

[2] Frisch SM, Schaller M and Cieply B. Mechanisms that link the oncogenic epithelial-mesenchymal transition to suppression of anoikis. J Cell Sci 2013; 126: 21-29.

[3] Schaller MD. Cellular functions of FAK kinases: insight into molecular mechanisms and novel functions. J Cell Sci 2010; 123: 1007-1013.

[4] Lietha D, Cai X, Ceccarelli DF, Li Y, Schaller MD and Eck MJ. Structural basis for the autoinhibition of focal adhesion kinase. Cell 2007; 129: 1177-1187.

[5] Brami-Cherrier K, Gervasi N, Arsenieva D, Walkiewicz K, Boutterin MC, Ortega A, Leonard PG, Seantier B, Gasmi L, Bouceba T, Kadaré G, Girault JA and Arold ST. FAK dimerization controls its kinase-dependent functions at focal adhesions. EMBO J 2014; 33: 356-370.

[6] Mitra SK, Hanson DA and Schlaepfer DD. Focal adhesion kinase: in command and control of cell motility. Nat Rev Mol Cell Biol 2005; 6: 56-68.

[7] Benes CH, Wu N, Elia AE, Dharia T, Cantley LC and Soltoff SP. The C2 domain of PKCdelta is a phosphotyrosine binding domain. Cell 2005; 121: 271-280.

[8] Casar B, Rimann I, Kato H, Shattil SJ, Quigley JP and Deryugina EI. In vivo cleaved CDCP1 promotes early tumor dissemination via complexing with activated beta1 integrin and induction of FAK/PI3K/Akt motility signaling. Oncogene 2014; 33: 255-268.

[9] Wright HJ, Arulmoli J, Motazedi M, Nelson LJ, Heinemann FS, Flanagan LA and Razorenova OV. CDCP1 cleavage is necessary for homodimerization-induced migration of triple-negative breast cancer. Oncogene 2016; 35: 4762-4772.

[10] Casar B, He Y, Iconomou M, Hooper JD, Quigley JP and Deryugina EI. Blocking of CDCP1 cleavage in vivo prevents Akt-dependent survival and inhibits metastatic colonization through PARP1-mediated apoptosis of cancer cells. Oncogene 2012; 31: 3924-3938.

[11] Pollan SG, Huang F, Sperger JM, Lang JM, Morrissey C, Cress AE, Chu CY, Bhowmick NA, You S, Freeman MR, Spassov DS, Moasser MM, Carter WG, Satapathy SR, Shah K and Knudsen BS. Regulation of inside-out beta1-integrin activation by CDCP1. Oncogene 2018; 37: 2817-2836.

[12] Bhatt AS, Erdjument-Bromage H, Tempst P, Craik CS and Moasser MM. Adhesion signaling by a novel mitotic substrate of src kinases. Oncogene 2005; 24: 5333-5343.

[13] Spassov DS, Baehner FL, Wong CH, McDonough S and Moasser MM. The transmembrane src substrate trask is an epithelial protein that signals during anchorage deprivation. Am J Pathol 2009; 174: 1756-1765.

[14] Alajati A, D'Ambrosio M, Troiani M, Mosole S, Pellegrini L, Chen J, Revandkar A, Bolis M, Theurillat JP, Guccini I, Losa M, Calcinotto A, De Bernardis G, Pasquini E, D'Antuono R, Sharp A, Figueiredo I, Nava Rodrigues D, Welti J, Gil V, Yuan W, Vlajnic T, Bubendorf L, Chiorino G, Gnetti L, Torrano V, Carracedo A, Camplese L, Hirabayashi S, Canato E, Pasut G, Montopoli M, Rüschoff JH, Wild P, Moch H, De Bono J and Alimonti A. CDCP1 overexpression drives prostate cancer progression and can be targeted in vivo. J Clin Invest 2020; 130: 2435-2450.

[15] Lin EY, Jones JG, Li P, Zhu L, Whitney KD, Muller WJ and Pollard JW. Progression to malignancy in the polyoma middle T oncoprotein mouse breast cancer model provides a reliable model for human diseases. Am J Pathol 2003; 163: 2113-2126.

[16] Spassov DS, Wong CH and Moasser MM. Trask phosphorylation defines the reverse mode of a phosphotyrosine signaling switch that under-

lies cell anchorage state. Cell Cycle 2011; 10: 1225-1232.
[17] Cooper LA, Shen TL and Guan JL. Regulation of focal adhesion kinase by its amino-terminal domain through an autoinhibitory interaction. Mol Cell Biol 2003; 23: 8030-8041.
[18] Goñi GM, Epifano C, Boskovic J, Camacho-Artacho M, Zhou J, Bronowska A, Martín MT, Eck MJ, Kremer L, Gräter F, Gervasio FL, Perez-Moreno M and Lietha D. Phosphatidylinositol 4,5-bisphosphate triggers activation of focal adhesion kinase by inducing clustering and conformational changes. Proc Natl Acad Sci U S A 2014; 111: E3177-3186.
[19] Loijens JC and Anderson RA. Type I phosphatidylinositol-4-phosphate 5-kinases are distinct members of this novel lipid kinase family. J Biol Chem 1996; 271: 32937-32943.
[20] van den Bout I and Divecha N. PIP5K-driven PtdIns(4,5)P2 synthesis: regulation and cellular functions. J Cell Sci 2009; 122: 3837-3850.
[21] Schill NJ and Anderson RA. Two novel phosphatidylinositol-4-phosphate 5-kinase type Igamma splice variants expressed in human cells display distinctive cellular targeting. Biochem J 2009; 422: 473-482.
[22] Schill NJ, Hedman AC, Choi S and Anderson RA. Isoform 5 of PIPKIgamma regulates the endosomal trafficking and degradation of E-cadherin. J Cell Sci 2014; 127: 2189-2203.
[23] Ling K, Doughman RL, Iyer VV, Firestone AJ, Bairstow SF, Mosher DF, Schaller MD and Anderson RA. Tyrosine phosphorylation of type Igamma phosphatidylinositol phosphate kinase by Src regulates an integrin-talin switch. J Cell Biol 2003; 163: 1339-1349.
[24] Jan YJ, Chen JF, Zhu Y, Lu YT, Chen SH, Chung H, Smalley M, Huang YW, Dong J, Chen LC, Yu HH, Tomlinson JS, Hou S, Agopian VG, Posadas EM and Tseng HR. NanoVelcro rare-cell assays for detection and characterization of circulating tumor cells. Adv Drug Deliv Rev 2018; 125: 78-93.
[25] Conze T, Lammers R, Kuci S, Scherl-Mostageer M, Schweifer N, Kanz L and Buhring HJ. CDCP1 is a novel marker for hematopoietic stem cells. Ann N Y Acad Sci 2003; 996: 222-226.
[26] Rotinen M, You S, Yang J, Coetzee SG, Reis-Sobreiro M, Huang WC, Huang F, Pan X, Yáñez A, Hazelett DJ, Chu CY, Steadman K, Morrissey CM, Nelson PS, Corey E, Chung LWK, Freedland SJ, Di Vizio D, Garraway IP, Murali R, Knudsen BS and Freeman MR. ONECUT2 is a targetable master regulator of lethal prostate cancer that suppresses the androgen axis. Nat Med 2018; 24: 1887-1898.
[27] Zarif JC, Lamb LE, Schulz VV, Nollet EA and Miranti CK. Androgen receptor non-nuclear regulation of prostate cancer cell invasion mediated by Src and matriptase. Oncotarget 2015; 6: 6862-6876.
[28] Sulzmaier FJ, Jean C and Schlaepfer DD. FAK in cancer: mechanistic findings and clinical applications. Nat Rev Cancer 2014; 14: 598-610.
[29] Serrels A, Lund T, Serrels B, Byron A, McPherson RC, von Kriegsheim A, Gómez-Cuadrado L, Canel M, Muir M, Ring JE, Maniati E, Sims AH, Pachter JA, Brunton VG, Gilbert N, Anderton SM, Nibbs RJ and Frame MC. Nuclear FAK controls chemokine transcription, tregs, and evasion of anti-tumor immunity. Cell 2015; 163: 160-173.
[30] Serrels B, McGivern N, Canel M, Byron A, Johnson SC, McSorley HJ, Quinn N, Taggart D, Von Kreigsheim A, Anderton SM, Serrels A and Frame MC. IL-33 and ST2 mediate FAK-dependent antitumor immune evasion through transcriptional networks. Sci Signal 2017; 10: eaan8355.
[31] You S, Knudsen BS, Erho N, Alshalalfa M, Takhar M, Al-Deen Ashab H, Davicioni E, Karnes RJ, Klein EA, Den RB, Ross AE, Schaeffer EM, Garraway IP, Kim J and Freeman MR. Integrated classification of prostate cancer reveals a novel luminal subtype with poor outcome. Cancer Res 2016; 76: 4948-4958.
[32] Putzke AP, Ventura AP, Bailey AM, Akture C, Opoku-Ansah J, Celiktaş M, Hwang MS, Darling DS, Coleman IM, Nelson PS, Nguyen HM, Corey E, Tewari M, Morrissey C, Vessella RL and Knudsen BS. Metastatic progression of prostate cancer and E-cadherin regulation by zeb1 and SRC family kinases. Am J Pathol 2011; 179: 400-410.
[33] Wortmann A, He Y, Christensen ME, Linn M, Lumley JW, Pollock PM, Waterhouse NJ and Hooper JD. Cellular settings mediating Src Substrate switching between focal adhesion kinase tyrosine 861 and CUB-domain-containing protein 1 (CDCP1) tyrosine 734. J Biol Chem 2011; 286: 42303-42315.
[34] Fraser M, Sabelnykova VY, Yamaguchi TN, Heisler LE, Livingstone J, Huang V, Shiah YJ, Yousif F, Lin X, Masella AP, Fox NS, Xie M, Prokopec SD, Berlin A, Lalonde E, Ahmed M, Trudel D, Luo X, Beck TA, Meng A, Zhang J, D'Costa A, Denroche RE, Kong H, Espiritu SM, Chua ML, Wong A, Chong T, Sam M, Johns J, Timms L, Buchner NB, Orain M, Picard V, Hovington H, Murison A, Kron K, Harding NJ, P'ng C, Houlahan KE, Chu KC, Lo B, Nguyen F, Li CH, Sun RX, de Borja R, Cooper CI, Hopkins JF, Govind SK, Fung C, Waggott D, Green J, Haider S, Chan-Seng-Yue MA, Jung E, Wang Z, Bergeron A, Dal Pra A, Lacombe L, Collins CC, Sahinalp C, Lupien M, Fleshner NE, He HH, Fradet Y, Tetu B, van der Kwast T, McPherson JD, Bristow RG

and Boutros PC. Genomic hallmarks of localized, non-indolent prostate cancer. Nature 2017; 541: 359-364.
[35] Thapa N, Choi S, Hedman A, Tan X and Anderson RA. Phosphatidylinositol phosphate 5-kinase Igammai2 in association with Src controls anchorage-independent growth of tumor cells. J Biol Chem 2013; 288: 34707-34718.
[36] Uekita T and Sakai R. Roles of CUB domain-containing protein 1 signaling in cancer invasion and metastasis. Cancer Sci 2011; 102: 1943-1948.
[37] Spassov DS, Wong CH, Harris G, McDonough S, Phojanakong P, Wang D, Hann B, Bazarov AV, Yaswen P, Khanafshar E and Moasser MM. A tumor-suppressing function in the epithelial adhesion protein Trask. Oncogene 2012; 31: 419-431.
[38] Uekita T, Jia L, Narisawa-Saito M, Yokota J, Kiyono T and Sakai R. CUB domain-containing protein 1 is a novel regulator of anoikis resistance in lung adenocarcinoma. Mol Cell Biol 2007; 27: 7649-7660.
[39] Ji L, Nishizaki M, Gao B, Burbee D, Kondo M, Kamibayashi C, Xu K, Yen N, Atkinson EN, Fang B, Lerman MI, Roth JA and Minna JD. Expression of several genes in the human chromosome 3p21.3 homozygous deletion region by an adenovirus vector results in tumor suppressor activities in vitro and in vivo. Cancer Res 2002; 62: 2715-2720.
[40] Spassov DS, Wong CH, Wong SY, Reiter JF and Moasser MM. Trask loss enhances tumorigenic growth by liberating integrin signaling and growth factor receptor cross-talk in unanchored cells. Cancer Res 2013; 73: 1168-1179.
[41] Le OT, Cho OY, Tran MH, Kim JA, Chang S, Jou I and Lee SY. Phosphorylation of phosphatidylinositol 4-phosphate 5-kinase gamma by Akt regulates its interaction with talin and focal adhesion dynamics. Biochim Biophys Acta 2015; 1853: 2432-2443.
[42] Li L, Kołodziej T, Jafari N, Chen J, Zhu H, Rajfur Z and Huang C. Cdk5-mediated phosphorylation regulates phosphatidylinositol 4-phosphate 5-kinase type I gamma 90 activity and cell invasion. FASEB J 2019; 33: 631-642.
[43] Jan YJ, Yoon J, Chen JF, Teng PC, Yao N, Cheng S, Lozano A, Chu GCY, Chung H, Lu YT, Chen PJ, Wang JJ, Lee YT, Kim M, Zhu Y, Knudsen BS, Feng FY, Garraway IP, Gao AC, Chung LWK, Freeman MR, You S, Tseng HR and Posadas EM. A circulating tumor Cell-RNA assay for assessment of androgen receptor signaling inhibitor sensitivity in metastatic castration-resistant prostate cancer. Theranostics 2019; 9: 2812-2826.
[44] Harrow J, Denoeud F, Frankish A, Reymond A, Chen CK, Chrast J, Lagarde J, Gilbert JG, Storey R, Swarbreck D, Rossier C, Ucla C, Hubbard T, Antonarakis SE and Guigo R. GENCODE: producing a reference annotation for ENCODE. Genome Biol 2006; 7 Suppl 1: S41-9.
[45] Dobin A, Davis CA, Schlesinger F, Drenkow J, Zaleski C, Jha S, Batut P, Chaisson M and Gingeras TR. STAR: ultrafast universal RNA-seq aligner. Bioinformatics 2013; 29: 15-21.
[46] Li B and Dewey CN. RSEM: accurate transcript quantification from RNA-Seq data with or without a reference genome. BMC Bioinformatics 2011; 12: 323.
[47] Zhai J, Lin H, Nie Z, Wu J, Cañete-Soler R, Schlaepfer WW and Schlaepfer DD. Direct interaction of focal adhesion kinase with p190RhoGEF. J Biol Chem 2003; 278: 24865-24873.
[48] Ikeda JI, Morii E, Kimura H, Tomita Y, Takakuwa T, Hasegawa JI, Kim YK, Miyoshi Y, Noguchi S, Nishida T and Aozasa K. Epigenetic regulation of the expression of the novel stem cell marker CDCP1 in cancer cells. J Pathol 2006; 210: 75-84.
[49] Adams MN, Harrington BS, He Y, Davies CM, Wallace SJ, Chetty NP, Crandon AJ, Oliveira NB, Shannon CM, Coward JI, Lumley JW, Perrin LC, Armes JE and Hooper JD. EGF inhibits constitutive internalization and palmitoylation-dependent degradation of membrane-spanning pro-cancer CDCP1 promoting its availability on the cell surface. Oncogene 2015; 34: 1375-1383.

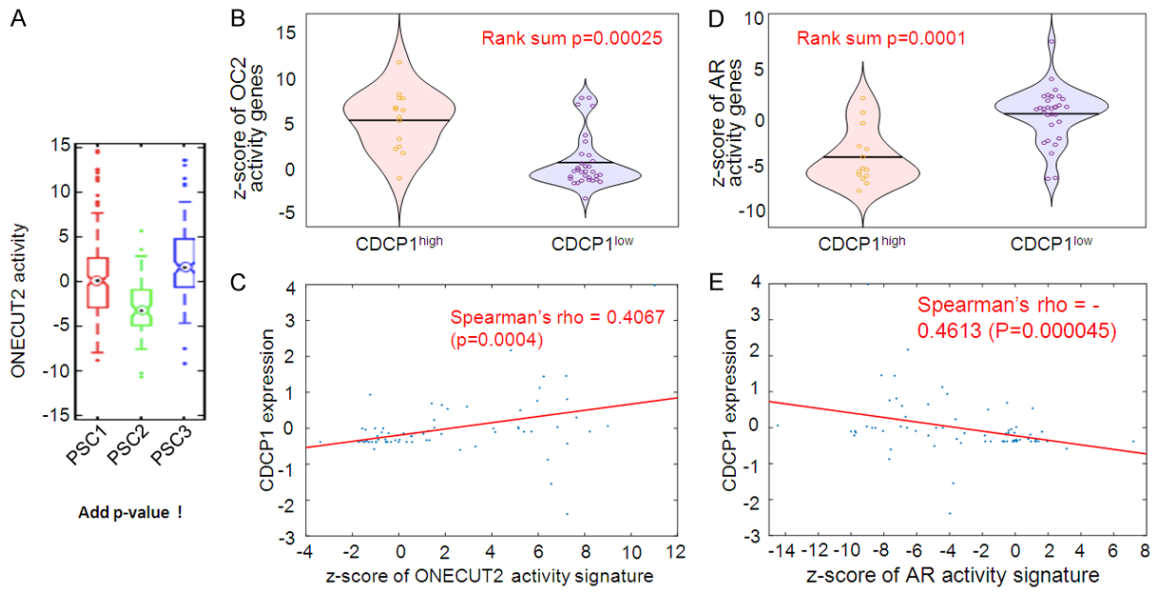

Figure S1. Relationship between CDCP1 mRNA expression, ONECUT2 and AR activities in primary, high-grade PCs. *CDCP1 and OC2 in primary, high-grade PCs.* A. OC2 activity across prostate cancer subtypes (PCS1-3) in the Gleason grade groups 4 and 5. The enrichment z-score of the OC2 signature was calculated and cases assigned to PCS1, PCS2 or PCS3 using a consensus signature score of genes differentially expressed in each subtype [54]. Bars indicate the 95th percentile. B and D. OC2 or AR activity in CDCP1^{high} versus low CDCP1^{low} high grade PCS3 cases (n = 72). C and E. Correlation between OC2 or AR activity z-scores and CDCP1 mRNA expression levels in high-grade PCS3.

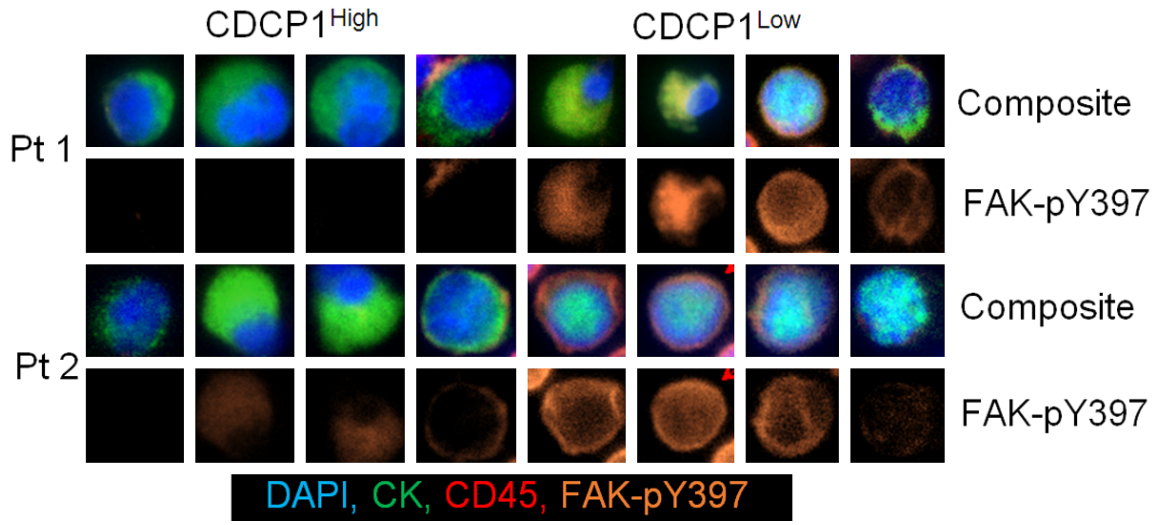

Figure S2. Kinase inhibitor treatment of the FAK activation network in detached DU145 and PC3 cells. Phospho-FAK-Y379 expression in CTCs from patients with mCRPC. Immunofluorescent staining of FAK-pY379 in CTC preparations from CDCP1^{High} and CDCP1^{Low} mCRPC patient subgroups. Cells were stained with DAPI, mouse anti-pan-cytokeratin, rat anti-CD45 and rabbit anti-FAK-pY379 and visualized with Alexa Fluor 488-conjugated anti-mouse, Alexa Fluor 555-conjugated anti-rabbit, and Alexa-647 donkey anti-rat antibodies.

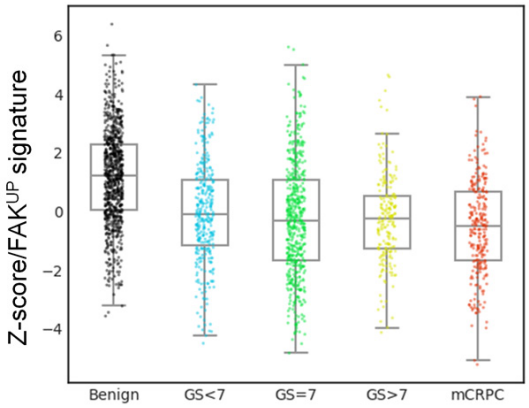

Figure S3. Time course of FAK-pY397 expression in detached, CDCP1^{Low} DU145 cells upon treatment with human plasma or BSA. FAK kinase activation signature in PC progression. The set of genes positively regulated by FAK (FAK^{UP}) was analyzed during PC progression. The genes in the panels are listed in Table S2.

Figure S4. Extracellular vesicles from DU145 CDCP1^{Low} cells do not activate FAK in the detached state. Time course of FAK-pY397 expression in detached, CDCP1^{Low} DU145 cells upon treatment with human plasma or BSA. CDCP1^{Low} DU145 cells were cultured in the detached state on HEMA coated plates in 10% human plasma or 1% BSA for the indicated time points. Western blots of whole cell lysates are probed for FAK-pY397 or FAK.

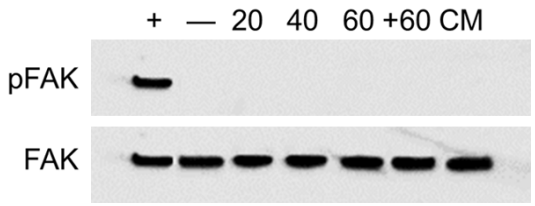

Figure S5. Confirmation of kinase inhibition by FAK, SRC and MEK inhibitory compounds. Extracellular vesicles from DU145 CDCP1^{Low} cells do not activate FAK in the detached state. Detached DU145 cells were treated for 3 hours with either FBS (+), 1% BSA (–), 20 ug, 40 ug or 60 ug protein from extracellular vesicles isolated from DU145 CDCP1^{Low} cells. A 3-hour treatment in conditioned media without vesicles (CM) is used as the control.

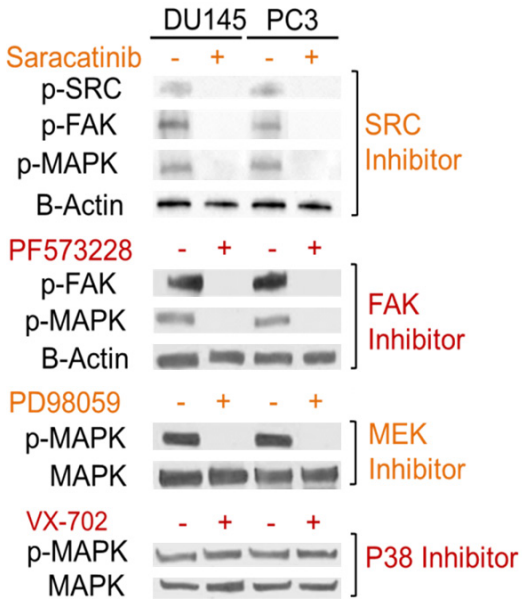

Figure S6. Loss of FAK-FAT domain activity does not affect FAK autophosphorylation in detached PC cells. Kinase inhibitor treatment of the FAK activation network in detached DU145 and PC3 cells. This figure shows that a 10 uM concentration of each inhibitor can effectively inhibit the kinase and its downstream pathway. Cell lysates from DU145 and PC3 cells were treated with Saracatinib, PF573228 (FAK inhibitor), PD98059 (MEK inhibitor) or VX-702 (p38 inhibitor) in the detached state for six hours and probed with anti-SRC-pY416, anti-FAK-pY379, anti-pMAPK42/44, MAPK or b-Actin controls. The inhibitors were all used at 10 uM concentration. The p38 inhibitors was used was used as a control.

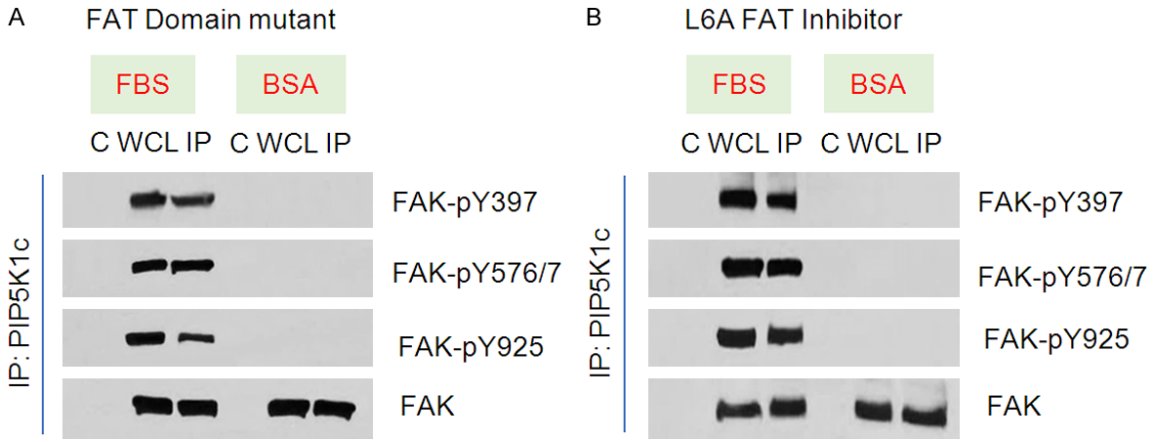

Figure S7. β1-Integrin, CDK5 or PIP5K1c complex formation with FAK-pY397 and FAK in the detached state is regulated by FCS. Loss of FAK-FAT domain activity does not affect FAK autophosphorylation in detached CDCP1^{Low} PC cells. A. FAT-null mutant does not induce FAK-pY397 expression in detached CDCP1^{high} DU145 cells. A mutant GFP-FAK protein missing the FAT domain was expressed in CDCP1^{high} DU145 cells. Immunoprecipitation using an anti-PIP5K1c antibody was used for isolation of FAK complexes. Western blots of FAK complexes are probed with anti-FAK-pY397 and FAK. Cab-control antibody precipitation, WCL-whole cell lysate, IP-PIP5K1c antibody precipitation. B. FAK-FAT mutant activity in CDCP1^{low} DU145 cells. The L6 FAT inhibitor or a FAK-FAT deletion mutant were used in CDCP1^{low} DU145 cells. Detached cells were treated with 10 uM L6A FAT inhibitor. FAK bound to PIP5K1c was precipitated and probed for FAK-pY397, pFAK-Y576/7 or FAK-pY925.

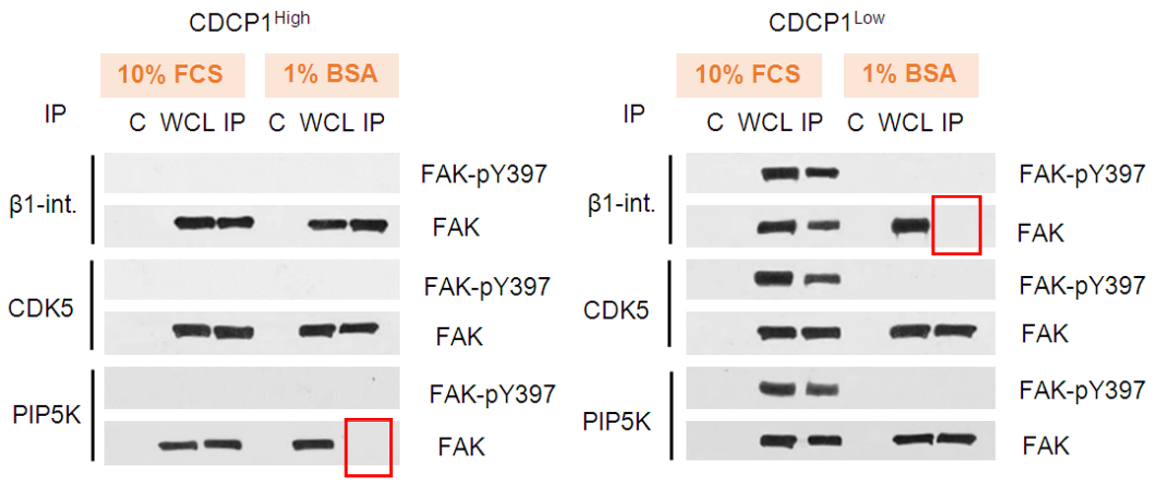

Figure S8. Talin/PIP5K1c complex formation in the detached state requires FCS. β1-Integrin, CDK5 or PIP5K1c complex formation with FAK-pY397 and FAK in the detached state is regulated by FBS. To determine the serum dependence of complex formation, CDCP1^{High} or CDCP1^{Low} DU145 cells were suspended in 10% FBS or 1% BSA for 3 hours. Antibodies to proteins indicated on the left of the WB were used for immunoprecipitation. WB were probed with FAK-pY397 and FAK. The red box marks the serum dependence of FAK complex formation with PIP5K1c in CDCP1^{High} cell and with beta1-integrin in CDCP1^{Low} cells, CDK5-FAK complexes are not sensitive to serum. C-IgG antibody control WCL-whole cell lysate IP-immunoprecipitation. The red box shows the absence of FAK in the β1-integrin complex, but inclusion of FAK in the CDK5 complex.

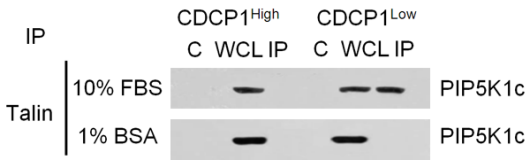

Figure S9. Talin/PIP5K1c complex formation in the detached state requires FBS. Talin-PIP5K1c complexes are visualized by co-immunoprecipitation of Talin and PIP5K from DU145 whole cell lysates. Detached CDCP1^{High} and CDCP1^{Low} DU145 cells are cultured in 10% FBS or 1% BSA for 3 hours and used in the immunoprecipitation experiments.

Table S1. Pollan et al.SCC_FAK-null_UP

Genes up-regulated in SCC FAK-null cells compared to SCC FAK-WT cells
IGFBP3
AKR1C3
CXCR4
SPRR1A
AGTR2
HEXB
OCIAD2
KRT20
TUSC1
ASGR1
OSR2
EPAS1
PMAIP1
LGALS7
CD302
TSPAN6
HUNK
ZNF518B
CYBA
SMOC2
KIAA1211L
CADM1
HTATIP2
SSLP1
NEFM
AKIP1
AKAP12
SLC14A1
ARL6IP1
NPNT
LOR
CEACAM1
FAM129A
WTIP
LTBP4
EID2
CXXC5
FBN2
B3GALTL
SOX4
NPR3
B4GALNT4
NT5DC2
KBTBD6
BHLHE22
GM26692
CPEB1
GATA6
TMEFF1
SOCS2
MEX3B
PLAC8
TRIQK

GM20632
TPMT
CBLB
DDAH2
LIFR
DNAJC12
FAM19A2
LRRC17
ISL1
DLL1
TRIM44
GAP43
SCX
PDGFRA
BTC
MGST1
VLDLR
CTSZ
CHD3
KLHL24
CA6
FAM117A
NTNG1
GFRA1
S100A16
TRAF5
TSHZ1
POGK
PKP1
IRX3
C14ORF28
CASD1
SGTB
GAS1
OASL2
HS6ST1
RIPK3
TGFB3
TTYH3
SAT2
DMP1
ENPP1
USP11
ATL1
HOXB8
SESN3
PTGFR
PCDHB12
PIH1D2
TIMP3
SAMD5
GATM
PMP22
RILPL1
TGFB1

CBR1
ZNF569
TMEM119
PCDHB17
RNF157
UBE2QL1
SHC4
SYNPO2
ITPKC
TMEM132A
PGF
TUFM
CREB5
PPM1H
IL18
SLC7A3
PRICKLE2
MAP1LC3A
CACNA1C
PCDH7
GLIPR2
LRRC10B
PELI2
C9ORF64
SDC3
S1PR1
LIMD2
RASL11B
UBE2D4
ITGB3
THSD4
MEX3A
MYL9
SYCE2
SRD5A3
TSHZ3
GM4992
CEP250
HOPX
RAB3B
GDA
KLRG1
SALL2

Table S2. Pollan et al.SCC_FAK-null_DN

Genes down-regulated in SCC FAK-null cells compared to SCC FAK-WT cells
DYNAP
CASP1
PLSCR2
CASP4
C1R
CES1G
CCL15
AQP5

CLDN9
CLDN6
ATG9B
ANGPT1
ZNF605
LDHB
PRSS23
GM2115
CYP2C18
KLHDC8A
MSLN
PLK2
CASP12
TNNT2
CA9
PAK3
C11ORF88
ANKRD1
TINAGL1
PSRC1
FABP4
ZFYVE26
IGF2BP1
PIK3CB
RHOX5
CRABP2
SLC35F3
STEAP1
ST7
SLC2A9
GPR149
ALS2CR12
FGFBP1
FAM198B
ZFPM2
SDPR
LHFP
GNG13
B3GNT3
ADAMTS1
TFPI
PDGFC
SLC19A2
ZNF182
APLN
PLCL2
HOXA10
PTPRK
PPARGC1B
MUM1L1
PLA2G16
VMN1R43
APOL7A
COL5A2

FAM212B
CCL5
NRP1
GMDS
ABCC4
GPR85
PHEX
S100A3
TUBD1
AJUBA
HIGD1A
CCDC126
ASPHD2
CDC42EP3
PLEKHA8
AKR1C13
CA5B
SMOC1
IRS1
FAT1
NDRG4
LURAP1L
GSTA4
LRP11
LPCAT4
SERPINB9B
IFIT1
PNPT1
FOXD1
METTL7A
ABCB1B
STYK1
PRKAR2B
DEFB41
PRELID2
RNF183
CADPS
AP4S1
C16ORF54
CSF1
PCCA
FLJ22184
MFAP3L
6230400D17RIK
LY75
9330151L19RIK
IL33
AK4
SSH2
KCNJ2
TCSTV1
STEAP2
FANCB
CA12